Localization and functional characterization of glutamate-gated chloride channels in the housefly *Musca domestica*

(イエバエにおけるグルタミン酸作動性クロルイオンチャネルの局在及び機能解析)

Tomo Kita

喜多　知

2014

Table of Contents

Abbreviations

1HEPS: 1-hydroxyethylphosphorothionate
BPB: 3-benzamido-*N*-phenylbenzamide
cl-LGIC: Cys-loop ligand-gated ion channel
CNS: central nervous system
cRNA: complementaryribonucleic acid
Ct: threshold cycle
DAPI: 4',6-diamidino-2-phenylindole
DMSO: dimethyl sulfoxide
DvGluT: *Drosophila* vesicular glutamate transporter
DvGluT: DvGluT gene
EBOB: ethynylbicycloorthobenzoate
EC_{50}: fifty percent effective concentration
GABA: γ-aminobutyric acid
GABACl: GABA-gated chloride channel
GluCl: glutamate-gated chloride channel
GluCl: GluCl subunit gene
HB: homogenization buffer
IC_{50}: fifty percent inhibitory concentration
LMN: large monopolar neuron
MdGluCl: *Musca domestica* glutamate-gated chloride channel
MdGluCl: MdGluCl subunit gene
MdRdl: *Musca domestica* GABA receptor
MdRdl: MdRdl gene
nAChR: nicotinic acetylcholine receptor
n_H: Hill coefficient
PBS: phosphate buffered saline
PBST: PBS containing 0.1% Tween 20
P buffer: 10 mM sodium phosphate buffer containing 300 mM NaCl
PMSF: phenylmethylsulfonyl fluoride
PS-14: 4-isobutyl-3-isopropylbicyclophosphorothionate
PTX: picrotoxinin
qPCR: quantitative PCR
Rdl: insect GABA receptor subunit named “resistance to dieldrin”

Rdl: Rdl subunit gene
RpS3: ribosomal protein subunit 3
RpS3: ribosomal protein subunit 3 gene
SDS: sodium dodecyl sulfate
SOS: standard oocyte solution
TBPS: *tert*-butylbicyclophosphorothionate
TEVC: two-electrode voltage clamp

Chapter 1

Introduction

Neurotransmitters

Neurons communicate with each other using signal molecules, neurotransmitters which are called ligands. Acetylcholine, L-glutamic acid (Fig. 1; hereafter glutamate) γ-aminobutyric acid (Fig. 1; hereafter GABA), and glycine are major fast neurotransmitters that act at ligand gated ion channels. Catecholamine such as adrenaline, noradrenaline, and dopamine play important roles not only as slow-acting neurotransmitters, but also hormones that act at G protein-coupled receptors (Hall, 1992). The fast neurotransmitters are stored in synaptic vesicles and released from the presynaptic terminals to the synaptic cleft. When the fast neurotransmitters bind to specific receptors on the postsynaptic membrane, the receptors are activated to increase ionic permeability through the membrane, leading to excitatory or inhibitory neurotransmission. The slow-acting neurotransmitters bind to receptors to produce second messengers within the target cells.

GABA and glutamate

Glutamate is an important amino acid known as a flavor ingredient and the constituent of protein. Glutamate is also important as a neurotransmitter and the precursor of the neurotransmitter GABA. In vertebrate fast neurotransmission, glutamate acts as an excitatory neurotransmitter, while GABA acts as an inhibitory neurotransmitter. However, in invertebrates such as insects, glutamate acts as both excitatory and inhibitory neurotransmitters (Cull-Candy and Usherwood, 1973; Cull-Candy, 1976; Delgado et al., 1989). GABA was first identified in the brain (Awapara et al., 1950) and found in the inhibitory neurons. GABA and glutamate bind to specific receptors, which include metabotropic and ionotropic receptors. Insect ionotropic GABA and glutamate receptors are categorized into Cys-loop ligand-gated ion channel family (cl-LGICs) and mediate fast inhibitory neurotransmission. It is interesting that the two closely-related amino acids share a common inhibitory neurotransmitter role in invertebrates.

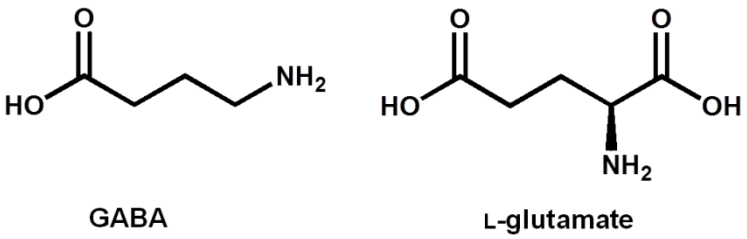

Fig. 1. Structures of GABA and L-glutamate.

Cys-loop ligand-gated ion channels (cl-LGICs)

The cl-LGICs play important roles in the communication between neurons, which is mediated by neurotransmitters. Acetylcholine-, GABA-, glutamate-, glycine-, histamine-, serotonin- and tyramine-gated chloride channels as well as acetylcholine-gated cation channels are members of this family (Cully et al., 1994, 1996; ffrench-Constant et al., 1993; Gisselmann et al., 2002; Marshall et al., 1990; Pirri et al., 2009; Putrenko, 2005; Ranganathan et al., 2000; Zheng et al., 2002). The receptors that belong to this family are formed by five subunits as homopentamer arranged to form an anion- or a cation-permeable pore at the center (Fig. 2; Jones and Sattelle, 2008; Ozoe, 2013). Each subunit has an N-terminal extracellular domain, which contributes to an orthosteric ligand-binding site, and four transmembrane α-helices (M1-M4), which form a channel domain. A Cys-loop in the N-terminal domain is characteristic of this family of receptors. Agonist binding to the orthosteric site induces the opening of the channel to enhance the membrane permeability to specific ions such as Na^+ and Cl^-. Amino acid residues at the -2' position in the second transmembrane (M2) domain are important for charge selectivity of the channels (Jensen et al., 2005). Invertebrate cl-LGICs represent targets of insecticides and anthelmintics.

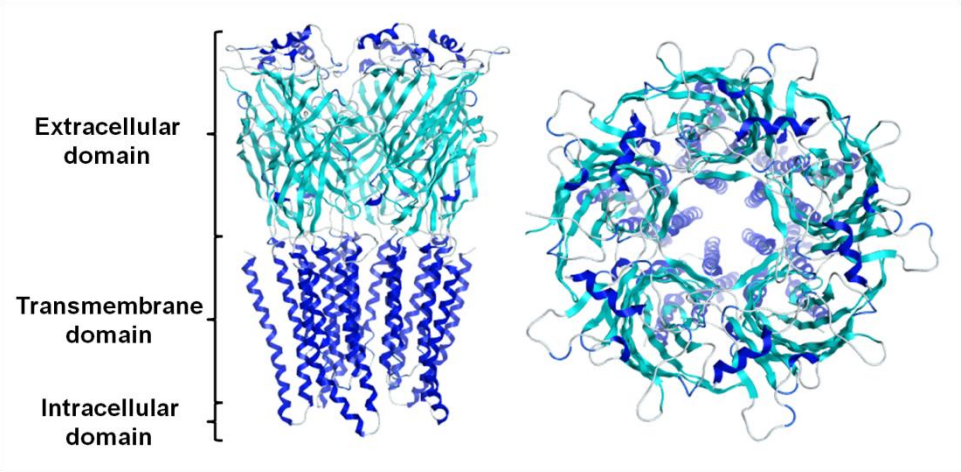

Fig. 2. Homology models of housefly glutamate-gated chloride ion channel.
This model was constructed using the X-ray crystal structure (PDB:3RIF) of *Caenorhabditis elegans* GluCl-α subunit as a template. The receptor is viewed from side (left) and from top (right). α-Helices are represented by cyan and β-sheets are represented by blue.

Insect GABA receptors

Two types of GABA receptors, ionotropic and metabotropic GABA receptors, are present in insects. Insect ionotropic GABA receptors are similar to vertebrate $GABA_A$ receptors in their function and structures. However, their pharmacological properties are different from those of vertebrate $GABA_A$ receptors. Insect ionotropic GABA receptors are sensitive to $GABA_A$ receptor antagonist picrotoxinin, but insensitive to bicuculline (Ozoe, 2013).

Three genes encoding GABA receptor subunits, Rdl, LCCH3, and GRD, were identified in *Drosophila melanogaster* (ffrench-Constant et al., 1991; Harvey et al., 1994; Henderson et al., 1993). Five Rdl subunits assemble to form functional pentameric GABA receptors. Homomeric LCCH3 or GRD failed to produce functional GABA receptors. LCCH3 and GRD formed a functional hereromeric GABA-gated cation channel when expressed in *Xenopus* oocytes (Gisselmann et al., 2004), but their physiological significance remains to be studied.

GABA-gated chloride channels (GABACls)

The inhibitory effect of GABA on the insect nervous system was first demonstrated in the metathoracic extensor tibiae muscles of the eastern lubber grasshopper (*Romalea microptera*) and the desert locust (*Schistocerca gregaria*)

(Usherwood and Grundfest, 1964, 1965). The cDNA encoding a subunit of the insect ionotropic GABA receptor was first cloned from *Drosophila melanogaster* (ffrench-Constant et al., 1991). The gene was termed *Rdl*. The *Rdl* orthologues have been identified from several insect species such as *Musca domestica* and *Tribolium castaneum* (Eguchi et al., 2006; Jones and Sattelle, 2007). Mutation of the Rdl subunit gene confers resistance to the cyclodiene insecticide dieldrin (ffrench-Constant et al., 1991). GABACls are important targets of phenylpyrazole, isoxazoline, and benzamide insecticides (Nakao et al., 2013; Ozoe, 2013; Ozoe et al., 2010). GABACls containing Rdl subunits belong to the cl-LGIC family.

Distribution of the Rdl subunit in insects has been reported. Rdl subunit is distributed in the medulla, the lobula and the lobula plate of the optic lobe, the fan-shaped body and the ellipsoid body of the central complex, the antennal lobe glomerulus, the α, β and γ lobes, the peduncle and calyx of the mushroom body of the brain, and the thoracic ganglia (Aronstein and ffrench-Constant, 1995; Enell et al., 2007; Harrison et al., 1996). Using an *Rdl*-Gal4 line, the Rdl subunit was suggested to be expressed in the large monopolar neuron (LMN) L4 and in a type of tangential neuron in the *Drosophila* lamina of the optic lobe (Kolodziejczyk et al., 2008). Using a double-labeling technique with cell-specific Gal4 drivers and *in situ Rdl* mRNA hybridization, the Rdl subunit was shown to be expressed in the majority of local interneurons and projection neurons that have cell bodies located within the antennal lobe glomerulus (Okada et al., 2009).

The Rdl subunit forms a homo-pentameric GABA-gated chloride channel (GABACl) (Eguchi et al., 2006; ffrench-Constant et al., 1993). GABA-induced currents are inhibited by noncompetitive antagonists such as picrotoxinin (PTX) and fipronil (Fig. 3) when expressed in *Xenopus* oocytes (Eguchi et al., 2006; Hosie et al., 1995; Ozoe et al., 2010).

The *Rdl* gene generates different transcripts called splice variant created by alternative splicing. Two variants of exon 3 and two variants of exon 6 were found in *Drosophila Rdl* gene, yielding four splice variants, Rdl_{ac}, Rdl_{ad}, Rdl_{bc} and Rdl_{bd}; channels containing a different variant differ in sensitivity to agonists and antagonists (ffrench-Constant and Rocheleau, 1993; Hosie et al., 2001). In addition, some pre-mRNA editing sites have been reported (Es-Salah et al., 2008; Jones et al., 2009). Pre-mRNA editing generates A or G nucleotide variations at specific sites, resulting in amino acid changes. It has been reported that some pre-mRNA changes alter sensitivity to GABA receptor antagonists (Es-Salah et al., 2008; Jones et al., 2009).

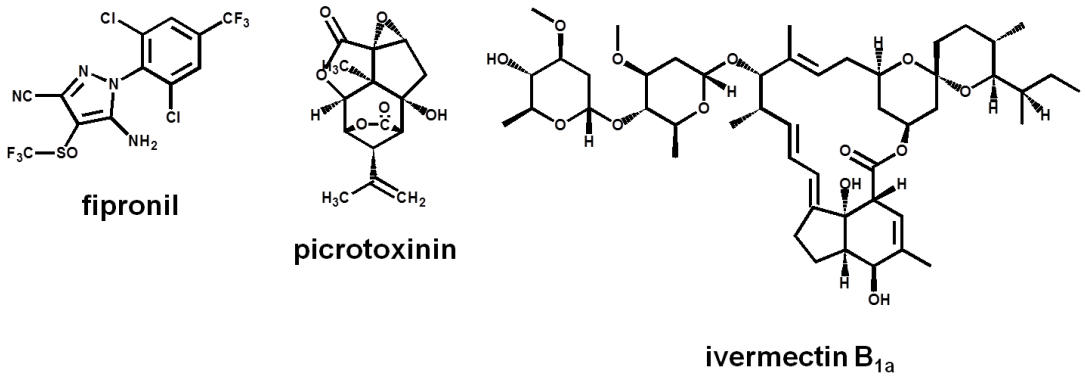

Fig. 3. Structures of the GABA receptor antagonists, fipronil and picrotoxinin, and the GluCl positive allosteric modulator, ivermectin B_{1a}.

Glutamate-gated chloride channels (GluCls)

The inhibitory action of glutamate was first observed as a hyperpolarization mediated by extrajunctional glutamate receptors in the extensor tibiae muscle of the metathoracic leg of *S. gregaria* (Cull-Candy and Usherwood, 1973). The two cDNAs encoding the α and β subunits of the inhibitory glutamate receptor were first cloned from *Caenorhabditis elegans* (Cully et al., 1994). The orthologous gene encoding the α subunit was subsequently cloned from *D. melanogaster* by the same group (Cully et al., 1996). Similar to the Rdl GABA receptors, the inhibitory glutamate receptor includes a homo- or hetero-pentameric chloride-permeable channel that is gated by the binding of glutamate (Cully et al., 1994, 1996). Therefore, it is referred to as the glutamate-gated chloride channel (GluCl). The cloning of the orthologous DNAs encoding GluCl subunits was described in several insect species (Cully et al., 1996; Eguchi et al., 2006; El Hassani et al., 2012; Janssen et al., 2007; Kwon et al., 2010). Although the physiological studies of GluCls in insects lag behind those of GABACls, GluCls have recently been implicated in several physiological functions such as the suppression of juvenile hormone biosynthesis (Liu et al., 2005) and olfactory memory (El Hassani et al., 2012). GluCls, which belong to the family of cl-LGICs, are composed of five subunits arranged to form a chloride-permeable pore at the center (Jones and Sattelle, 2008; Ozoe, 2013).

Insect GluCls serve as a target of insecticides such as avermectins and fipronil (Kane et al., 2000; Kwon et al., 2010; Zhao et al., 2004b). Glutamate-induced currents are inhibited by GABA receptor antagonists and are potentiated by ivermectin (Fig. 3). The macrocyclic anthelmintic ivermectin is widely used for the control of parasitic

nematodes. An X-ray crystallography study of a homomeric GluCl-α channel from *C. elegans* revealed the location of the binding sites for ligands, such as glutamate, ivermectin B_{1a}, and PTX (Hibbs and Gouaux, 2011).

The housefly

The housefly (*Musca domestica* L.) belongs to the order Diptera, and widely found all over the world. The houseflies are sanitary insects, which carry serious diseases, such as salmonellosis, typhoid fever and cholera (Højland et al., 2013). To facilitate studies on houseflies, genome sequences were analyzed (Scott et al., 2009). Several classes of insecticides such as organophosphates, carbamates, pyrethroids, and new insecticides are used for their management (Khan et al, 2013). Development of insecticide resistance is an important problem. It is important to investigate their neurotransmitter receptors, which are target of insecticides for controlling insect pests.

The objectives of study

GABACls and GluCls have similar structures and functions. These receptors represent the targets of insecticides such as fipronil and abamectin. Although the pharmacological properties of these channels have been reported (Ozoe, 2013), little is known about the physiological roles of these receptors. Therefore, I first investigated the localization of GluCls in the housefly and compared with GABACls to understand differences in their physiological roles (Chapter 2). I also investigated gene expression of splice variants using quantitative reverse transcription PCR (qRT-PCR) and the pharmacological properties of channels consisting of the variants using two electrode voltage clamp (TEVC) (Chapter 3). The effects of a few insecticidal GABA antagonists on GluCls were also examined (Chapter 4).

Chapter 2

Differential distribution of glutamate- and GABA-gated chloride channels

Introduction

Glutamate functions as an excitatory neurotransmitter, while GABA is an inhibitory neurotransmitter. However, in invertebrates such as insects, glutamate acts as both excitatory and inhibitory neurotransmitters (Cull-Candy, 1976; Cull-Candy and Usherwood, 1973; Delgado et al., 1989). Glutamate is the precursor of the biosynthesis of GABA. It is interesting that the two closely-related amino acids share an inhibitory neurotransmitter role in invertebrates.

The molecular function and pharmacology of GluCls have recently been well studied (Eguchi et al., 2006; Janssen et al., 2010; Narahashi et al., 2010), but not much is known about the physiology and localization of GluCls in the insect body, particularly, in terms of comparison with that of GABACls. While the coexpression of GABACls and GluCls in a single neuron has been reported in some cases (Barbara et al., 2005; Cayre et al., 1999; Ihara et al., 2005; McCarthy et al., 2011), I am interested in determining whether there are differences in their physiological roles as two similar channels are used for the same inhibitory role. In this chapter, I thus investigate the transcript and protein expression levels of the GluCl and Rdl subunits in several tissues at various developmental stages of the housefly. I also examine the tissue distribution of the GluCl protein in the adult fly and compare it to the distribution of the Rdl protein using immunohistochemical staining. Here I describe a differential distribution of GluCls and GABACls in the housefly.

Materials and methods

RNA isolation and cDNA synthesis

The WHO/SRS strain of houseflies (*Musca domestica* L.) was used throughout the study. Total RNA was isolated from the heads, thoraces, abdomens and legs of male

adults (2-3 days after eclosion) using Isogen (Wako). Total RNA was also isolated from the head parts of pupae (1 day after pupation), larvae (3-4 days after hatching), and embryos. First-strand cDNA was synthesized from gDNA Eraser-treated total RNA (1 μg) by priming with oligo-dT primers and random 6-mers using the PrimeScript® RT Reagent Kit (Takara).

qPCR

qPCR was performed with a Thermal Cycler Dice Real Time System (Takara) using cDNA prepared from 10 ng of total RNA, THUNDERBIRD™ SYBR® qPCR Mix (Toyobo), and gene specific primers. The primers MdG-83F (5'-ACAGTGTACAGCTAACATTCC-3') and MdG-118GR (5'-AACAAATCAGGCATCCAG-3') were used to amplify the gene (*MdGluCl*) encoding the *M. domestica* GluCl (MdGluCl) subunit (accession no. AB177546). The primers MdR-123RF (5'-CTGGTGTAGAAACACTATCGG-3') and MdR-162RR (5'-ATTCGTTACTGGTTGTTGC-3') were used to amplify the gene (*MdRdl*) encoding the *M. domestica* Rdl (MdRdl) subunit (accession no. AB177547). The PCR program consisted of 95 °C for 30 s for initiation, 40 cycles of 95 °C for 5 s and 58 °C for 30 s, followed by 95 °C for 15 s, 58 °C for 30 s and 95 °C for 15 s for the dissociation curve analysis. The specific amplification was assessed by electrophoresis of the PCR products using a 4% agarose gel and melting curve analysis. The expression levels of transcripts were normalized using those of the transcript of ribosomal protein subunit 3 (*RpS3*) as an internal control, which showed acceptable variability among samples from different tissues, with threshold cycle (C_t) values of <1.5. The primers Md-RPS3_F (5'-AAGCTGAATCTCTCCGTTAC-3') and Md-RPS3_R (5'-GACGACGACTTCACAGC-3') were used to amplify *RpS3* (accession no. AF207603).

Radioligand binding experiments

The heads, abdomens, or thoraces of 100 adult male houseflies (2-5 days after eclosion) were homogenized in 10 mM Tris-HCl buffer (pH 7.5) containing 0.25 M sucrose and 0.5 mM phenylmethylsulfonyl fluoride (PMSF) using a Teflon-glass homogenizer. The P_2 membrane was prepared as previously described (Ju et al., 2010). The membrane pellets were suspended in the assay buffers described below and immediately used for the binding experiments.

The membrane homogenate (40 μg protein) was incubated with 1.0 nM [^{3}H]milbemycin A_4 (16 Ci/mmol) for 60 min at 22 °C in 0.5 ml of 50 mM HEPES buffer containing 0.02% Triton X-100 (pH 7.4) to determine the total binding. Nonspecific binding was determined in the presence of 1 μM milbemycin A_4. The membrane homogenate (200 μg protein) was incubated with 0.5 nM [^{3}H]EBOB (30 Ci/mmol; PerkinElmer) for 70 min at 22 °C in 1.0 ml of 10 mM sodium phosphate buffer containing 300 mM NaCl (pH 7.5; P buffer) to determine the total binding. Nonspecific binding was determined in the presence of 1 μM α-endosulfan. After incubation, the mixtures were filtered through Whatman GF/B filters and washed twice with 5 ml of cold (10 °C) water containing 0.1% Triton X-100 ([^{3}H]milbemycin A_4) or P buffer ([^{3}H]EBOB) using a Brandel M-24 cell harvester. The filters were pre-immersed in 50 mM HEPES buffer containing 0.1% polyethylenimine (pH 7.4) ([^{3}H]milbemycin A_4) or P buffer ([^{3}H]EBOB). The radioactivity on the filter was counted in a toluene/2-methoxyethanol-based scintillation fluid using a Beckman LS 6000 SE scintillation spectrometer.

Preparation of antibodies

Antibodies were prepared by Sigma-Aldrich Japan (Tokyo). Antisera for the MdGluCl and MdRdl subunits were raised against peptide sequences at the C-terminus of the subunits, which were C+S_{446}TYLFREEEDETF$_{458}$ (accession no. AB177546) and C+H_{560}VSDVVADDLVLLGEEK$_{576}$ (accession no. AB177547), respectively. These peptides were conjugated with bovine serum albumin. The antigens were injected into rabbits. The antiserum for MdGluCl was purified using a column with the antigen peptide.

Western blotting

Housefly head membranes were prepared as described above. The membranes were then suspended in PBS containing 1% Triton X-100. After incubation on ice for 30 min, the suspension was centrifuged for 30 min at 25,000*g*. The resulting pellet was suspended in Laemmli buffer and boiled for 5 min at 96 °C. The lysate was loaded onto a 7.5% SDS-polyacrylamide gel with a 5% stacking gel. After SDS-PAGE, the proteins were transferred to a PVDF membrane (Immobilon^{TM}-P, Merck Millipore). The membrane was incubated in PBS containing 0.1% Tween 20 (PBST) supplemented with 5% nonfat dried milk (blocking buffer) for 1 h at room temperature.

The PVDF membrane was incubated for 2 h at 37 °C with the purified anti-MdGluCl antibody (2.2 mg/ml) or anti-MdRdl antiserum at a dilution of 1:1000 in the blocking buffer. The PVDF membrane was washed with PBST three times and then incubated for 1 h at 37°C with stabilized peroxidase-conjugated goat anti-rabbit IgG (H+L) (Pierce; 10 μg/ml) diluted 1:500 with PBST. The chemiluminescence was detected with SuperSignal® West Femto Maximum Sensitivity Substrate (Pierce) using an ImageQuant LAS 4000 imager (GE Healthcare).

Immunohistochemistry

Adult male houseflies (2-5 days after eclosion) were dissected in a Bouin fixative solution at room temperature. After fixation for 15-18 h at 4 °C, the tissues were dehydrated through a graded ethanol series, cleared, and embedded in Histosec® pastilles (without DMSO) (Merck KGaA). The embedded tissues were sliced into 10-20 μm-thick sections. The sections were placed onto APS-coated clean glass slides and allowed to dry at 40 °C overnight. The sections were then deparaffinized in xylene and rehydrated through an ethanol series into PBS. The tissue sections were incubated in PBS containing 10% normal goat serum for 2 h at room temperature. The blocking serum was removed and the tissues were covered with a primary antibody diluted in PBS containing 10% normal goat serum. The slides were incubated for 2 h at 37 °C or overnight at 4 °C. The purified anti-MdGluCl antibody and anti-MdRdl antiserum were diluted 1:1500 with PBS containing 10% normal goat serum. In the control experiments, antibodies preabsorbed with the antibody-raising peptide were used as the primary antibody. After three PBS washes, the tissues were incubated for 1 h at 37 °C with an Alexa Fluor 488® goat anti-rabbit IgG (H+L) (Invitrogen) secondary antibody. The tissues were then washed, mounted, and stained with DAPI using VECTASHIELD® (Vector Laboratories). The mounted tissues were viewed with a Leica TCS SP5 confocal microscope. The confocal images were processed with LAS AF software (Leica) and edited for brightness and contrast with Adobe Photoshop CS5 Extended software.

Results

Expression of MdGluCl and MdRdl transcripts in tissues and at developmental stages

I first investigated the transcription of the genes *MdGluCl* and *MdRdl* in different

tissues and at different developmental stages using qPCR. *MdGluCl* and *MdRdl* were predominantly expressed in the adult head (Fig. 4A). The *MdGluCl* and *MdRdl* transcription levels were approximately equivalent in the head. Although these genes were also expressed in the thorax and abdomen, the levels in these regions were reduced compared to the head. The thoraces without legs and wings had low levels of both transcripts. It should be noted that *MdGluCl* had higher transcription levels than *MdRdl* in the leg. The MdGluCl and MdRdl transcript levels in the larval and pupal heads were lower than those in the adult head. The transcripts of both genes in embryos were undetectable.

Expression of GluCl and GABACl proteins in adult tissues

I next examined the expression of GluCls and GABACls in the tissues of the adult using ligand-binding experiments with specific, high-affinity probes for these channels (Ozoe, 2013). High levels of specific binding of [^{3}H]milbemycin A_4, a positive allosteric modulator of GluCls, and [^{3}H]EBOB, a noncompetitive GABA receptor antagonist, occurred in the head membranes of the adult (Fig. 4B,C). The specific binding of these radioligands to thorax membranes was lower than that to the head membranes. The specific binding of the two ligands to the abdominal membranes was marginal.

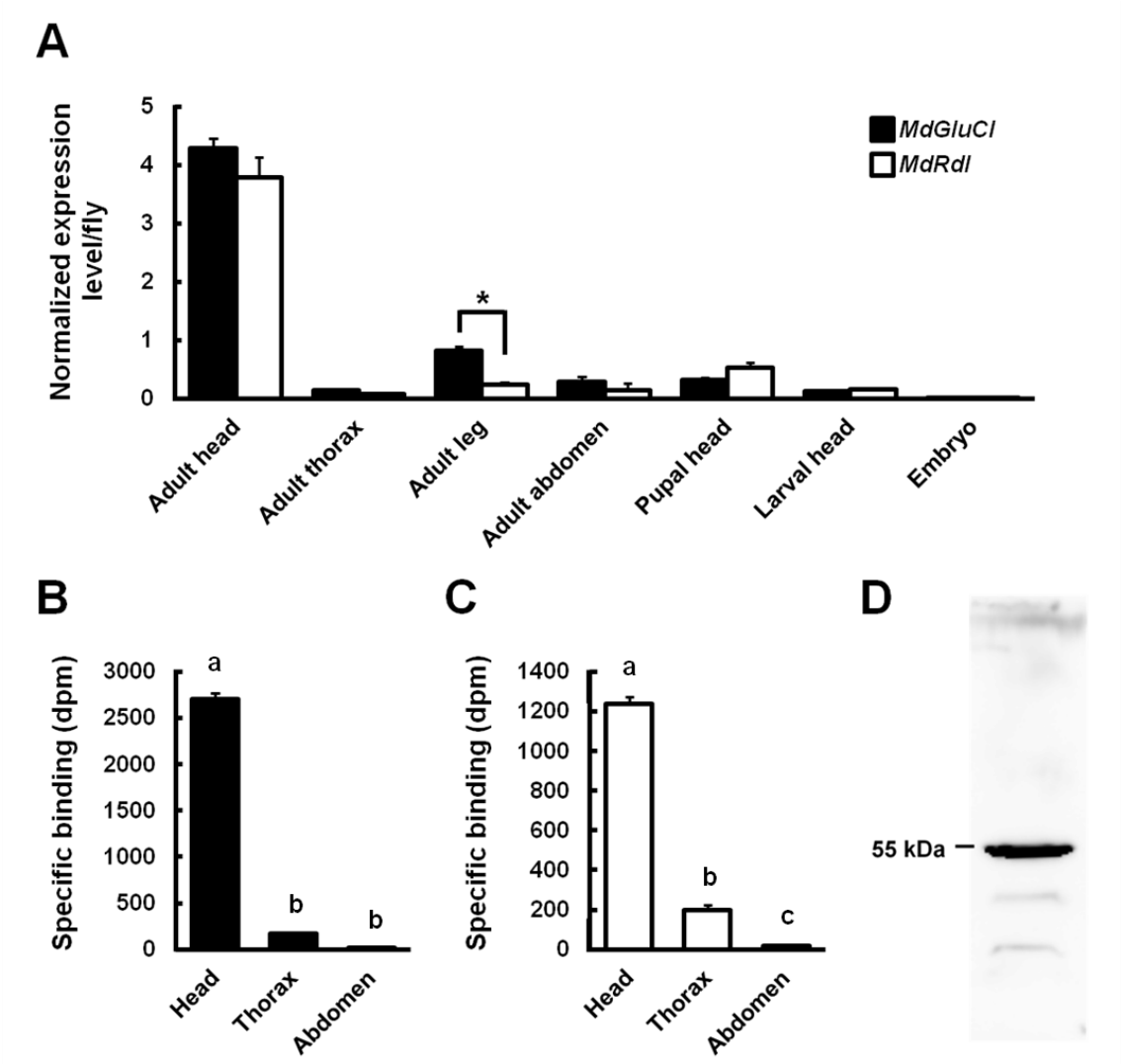

Fig. 4. Expression levels of GluCls and GABACls according to the developmental stages and body parts of houseflies. The data in A-C are means ± SEM (n = 3). (A) qPCR determination of MdGluCl and MdRdl transcript levels. The results are normalized relative to the internal control *RpS3*. * P<0.01 by unpaired *t*-test. (B,C) GluCl and GABACl levels determined by radioligand binding to membranes from body parts. Specific [^{3}H]milbemycin A_4 binding/40 μg protein and specific [^{3}H]EBOB binding/200 μg protein are presented in B and C, respectively. Different letters above the bars indicate significant differences (P<0.05 by one-way ANOVA followed by Bonferroni-Dunn post-hoc test). (D) Western blot of head homogenates with an anti-MdGluCl antibody.

Tissue distribution of GluCl and Rdl subunits in the adult

qPCR and radioligand binding results showed that the GluCls and GABACls were

highly expressed in adult tissues. Therefore, I examined the tissue distribution of the GluCl and Rdl subunits in the adult using polyclonal antibodies raised against C-terminal peptides derived from these proteins. The purified anti-MdGluCl antibody recognized a protein of 52 kDa, which corresponds to the predicted size of the MdGluCl subunit (Fig. 4D). To investigate the specificity of the antibodies, MdGluCl and MdRdl peptide-preabsorbed antibodies were used as the primary antibody in immunohistochemistry. The preabsorbed antibodies showed no specific immunostaining and nonspecific staining was scarcely detected (Figs. 5A and 6A). These results suggest that the two antibodies are specific for their corresponding subunits.

Immunostaining in the adult head

Frontal sections through the adult head showed specific staining of MdGluCl in several regions of the optic lobe (Fig. 5). Intense staining was highlighted in the lamina, which is the first neuropil of the optic lobe. Specific staining was present in the neuropil containing the cartridge but not in the cell bodies of monopolar neurons (Fig. 5D). Furthermore, specific MdGluCl staining was detected in several layers of the outer medulla, the retina basement membrane, and the pigment cells beneath the lens.

In the brain, MdRdl staining was observed in the ellipsoid body of the central complex (Fig. 6B). Additional staining was found in the α, β and γ lobes, the peduncle of the mushroom body, and the antennal lobe (Fig. 6C). Significant MdGluCl staining was not detected in these regions of the brain (data not shown). Although specific MdRdl staining was detected in several layers of the medulla, the lobula, and the lobula plate (Fig. 6D), only weak staining was detected in the lamina.

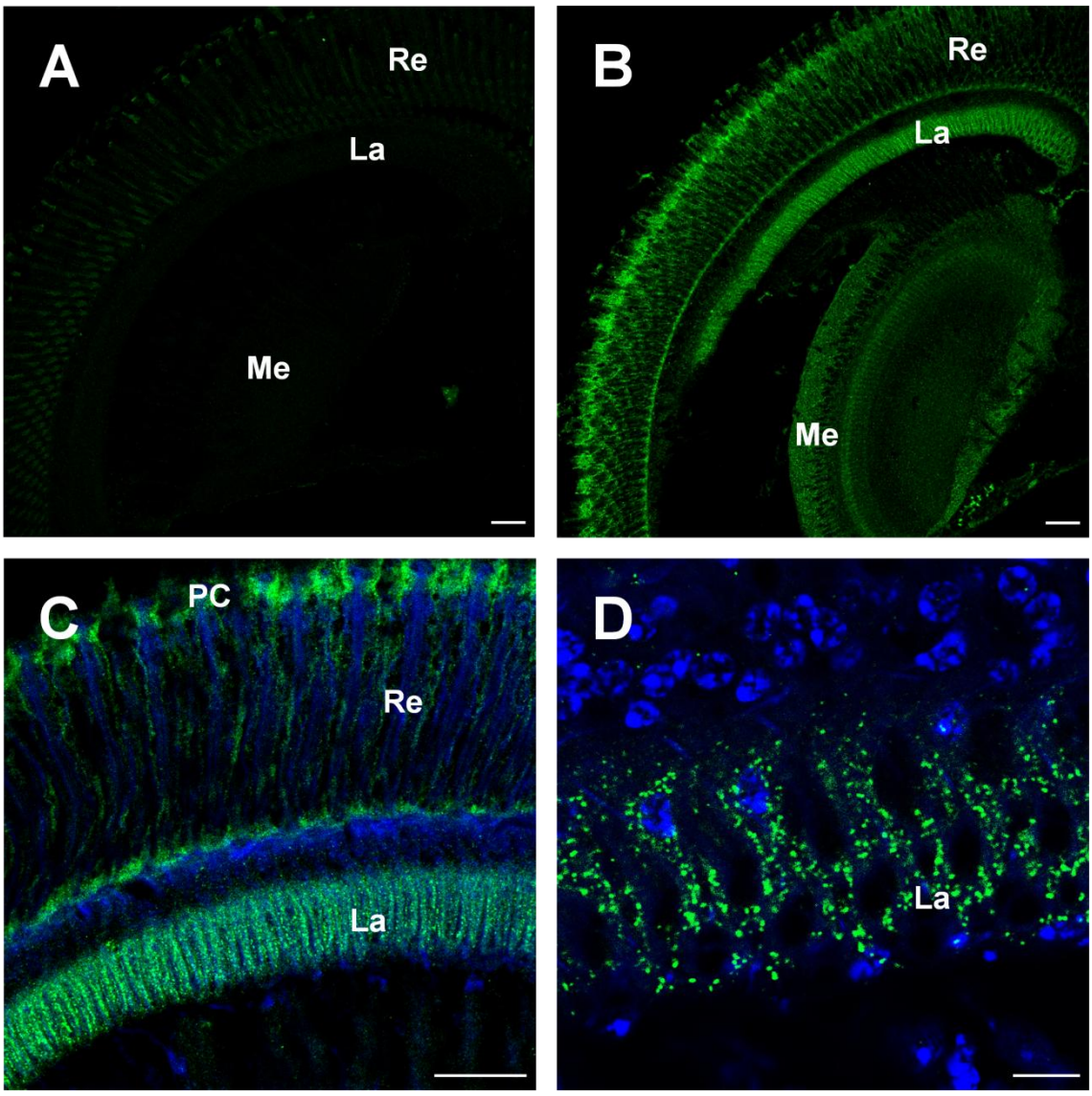

Fig. 5. MdGluCl immunostaining in the frontal section through the adult head. (A) Control staining with antibody preabsorbed with the C-terminus peptide conjugate in the optic lobe. La, lamina; Me, medulla; Re, retina. (B) MdGluCl immunostaining (green) in the optic lobe. (C) Magnification of the retina and the lamina neuropil. PC, pigment cell. (D) Higher magnification of the lamina. Note that the cell bodies of monopolar cells are stained by DAPI (blue) but not by the antibody. Scale bar: 50 μm in A, B, and C; 10 μm in D.

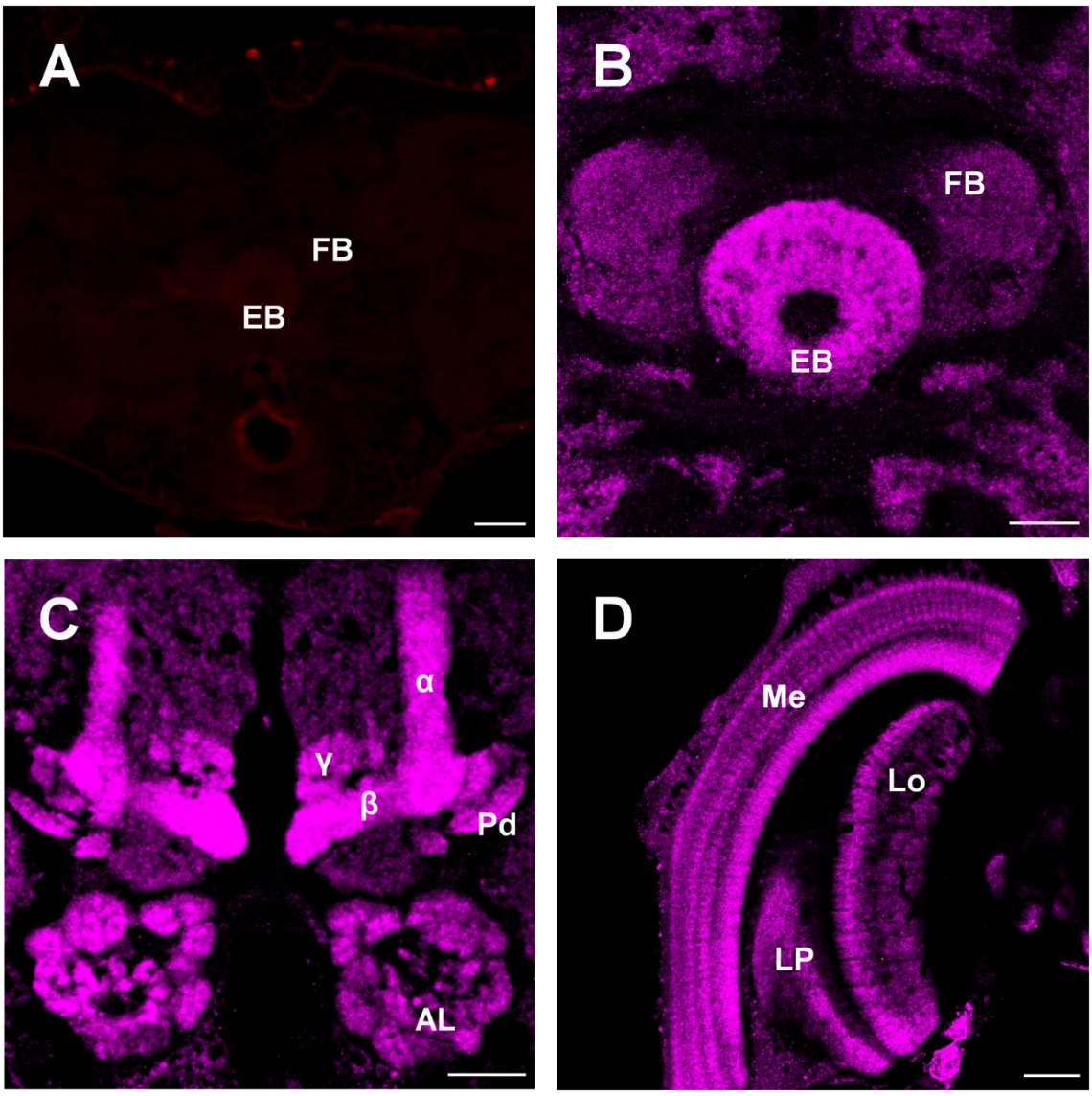

Fig. 6. MdRdl immunostaining in the frontal section through the adult head. (A) Control staining with antiserum preabsorbed with the C-terminus peptide conjugate in the central complex. EB, ellipsoid body; FB, fan-shaped body. (B) The central complex. (C) The mushroom body and antennal lobe. α, α lobe; AL, antennal lobe; β, β lobe; γ, γ lobe; Pd, peduncle. (D) The optic lobe. Lo, lobula; LP, lobula plate; Me, medulla. Scale bar: 50 μm in A, C, and D; 25 μm in B.

Immunostaining in the adult thorax and leg

Horizontal sections through the thorax displayed MdGluCl and MdRdl staining in the ganglion (Fig. 7A,B,D,E). However, a difference in the two staining patterns was evident. MdGluCl staining was located in the monopolar cell bodies of motor neurons (Fig. 7A,B). In contrast, MdRdl staining was widely detected in the thoracic ganglia

and most likely included the cell bodies of motor neurons (Fig. 7D,E). MdGluCl staining was also observed along the femoral muscle of the prothoracic leg (Fig. 7C), whereas MdRdl staining was undetectable in the femur (Fig. 7F).

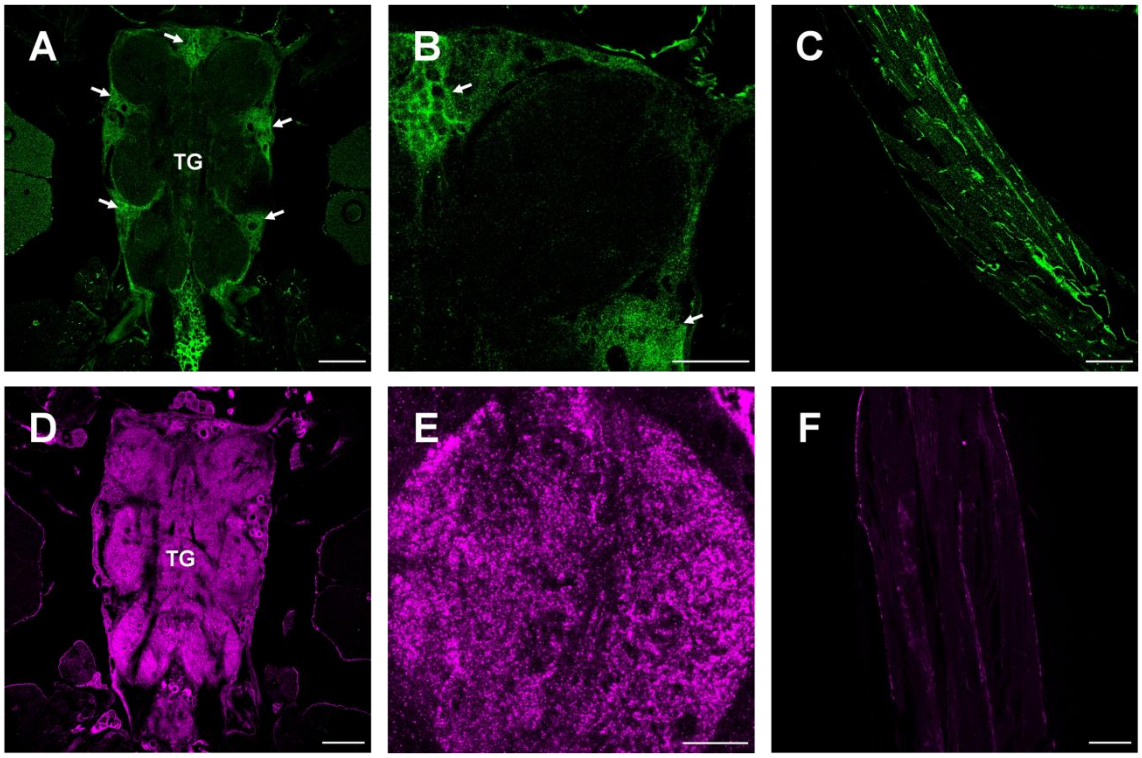

Fig. 7. MdGluCl (green) and MdRdl immunostaining (magenta) in the horizontal section through the thoracic ganglion and the prothoracic leg. (A,D) The thoracic ganglion. The arrows indicate the cell bodies of motor neurons. TG, thoracic ganglion. (B,E) Magnification of the first thoracic ganglion. (C,F) The femur of the prothoracic leg. Scale bar: 100 μm in A, C, D, and F; 50 μm in B; 25 μm in E.

Discussion

GluCls and GABACls play key roles in inhibitory neurotransmission in the nervous systems of insects and represent major targets of insecticides (Ozoe, 2013). In the present study, I first compared the expressions of the transcript and protein of GluCls with those of GABACls (Rdl) in the housefly by qPCR and radioligand-binding experiments. The results show that GluCls and GABACls are equally abundant in the adult head (Fig. 4). This most likely reflects the abundance of the specialized nerve tissues in the head compared to other parts. Although GABACls and GluCls are indeed present in adolescent flies (Bloomquist, 1994; Enell et al., 2007;

Lee et al., 2003; Zhang et al., 1994), our data indicate that these receptors are expressed at much lower density than in adults. Apart from their localization in the central nervous system, it is interesting to note that the MdGluCl transcript is more highly expressed than the MdRdl transcript in the leg (Fig. 4A). The high level of MdGluCl expression in the leg could be related to the fact that GluCls were first identified as extrajunctional H (hyperpolarization)-receptors on the leg muscle fiber membrane of *S. gregaria* (Cull-Candy and Usherwood, 1973).

To examine the differences in the distribution of GluCls and GABACls in adult houseflies more precisely, I next performed immunohistochemical analysis using specific antibodies. Frontal sections through the adult head showed that MdRdl staining was located in several regions of the brain. Intense MdRdl immunostaining was observed in the antennal lobe, the α, β and γ lobes, and the peduncle of the mushroom body using specific antibodies (Fig. 6C). These areas are associated with olfactory learning and memory. Moreover, MdRdl staining was detected in the ellipsoid body of the central complex, which is a center for sensory integration (Fig. 6B). Intense staining with anti-MdRdl serum was evident in the medulla, the lobula, and the lobula plate of the optic lobe, whereas only weak staining was detected in the lamina (Fig. 6D). This indicates the involvement of GABACls in the visual pathways.

Previous immunohistochemical analyses using *Drosophila* indicated that the Rdl subunit is distributed in the medulla, the lobula and the lobula plate of the optic lobe, the fan-shaped body and the ellipsoid body of the central complex, the antennal lobe glomerulus, the α, β and γ lobes, the peduncle and calyx of the mushroom body of the brain, and the thoracic ganglia (Aronstein and ffrench-Constant, 1995; Enell et al., 2007; Harrison et al., 1996). Using an *Rdl*-Gal4 line, the Rdl subunit was suggested to be expressed in the large monopolar neuron (LMN) L4 and in a type of tangential neuron in the *Drosophila* lamina of the optic lobe (Kolodziejczyk et al., 2008). Using a double-labeling technique with cell-specific Gal4 drivers and *in situ Rdl* mRNA hybridization, the Rdl subunit was shown to be expressed in the majority of local interneurons and projection neurons that have cell bodies located within the antennal lobe glomerulus (Okada et al., 2009). The Rdl localization in houseflies generally accords with that in fruit flies.

Our immunostaining results show that GluCls are located in the lamina and outer medulla of the optic lobe and the retina in the housefly (Fig. 5). Intense GluCl staining was observed in the lamina neuropil but not in the cell bodies of monopolar cells. This is in marked contrast to intense staining in the medulla, the lobula, and the lobula plate of the optic lobe with anti-MdRdl serum. These findings suggest that GluCls and

GABAClS play a different role in the regulation of visual information in the housefly.

In the insect visual system, the optic lobe beneath the retina consists of four neuropil layers: the lamina, medulla, lobula, and lobula plate (Sinakevitch and Strausfeld, 2004). The lamina contains a cartridge in which the photoreceptor axons surround the LMNs L1 and L2 and provide synaptic inputs. The L1 and L2 neurons are involved in the mediation of motion-based vision. The cell bodies are located above the lamina neuropils and receive signals from photoreceptor cells. These neurons send signals to the medulla by extending their axons. Glutamate-like immunoreactivity was identified in the L1-L3 neurons in the common green bottle fly (*Phaenicia sericata*) (Sinakevitch and Strausfeld, 2004), although a study that examined glutamatergic neurons using an antibody against the vesicular glutamate transporter of *Drosophila* (DvGluT) and a Gal4 driver of DvGluT indicated that the expression of DvGluT (a marker protein of glutamatergic neurons) was not recognized in the L1-L3 terminals in the medulla (Daniels et al., 2008). Using antisera against glutamate and DvGluT, immunostaining was detected in the α-processes of the lamina amacrine neurons and the L2 neurons of *Drosophila* (Kolodziejczyk et al., 2008). In addition, neurons that release glutamate in the *Drosophila* visual system were recently identified using a Gal4 driver of DvGluT (Raghu and Borst, 2011). These neurons included the L2 neurons. Real-time PCR analysis of L1 and L2 cell bodies dissociated from the *Drosophila* lamina showed that the *DvGluT* transcript was detected in L1 neurons (Takemura et al., 2011). Although these findings indicate that the L1 or L2 neurons are glutamatergic, whether glutamate acts as an excitatory or inhibitory neurotransmitter has remained unclear. Our findings suggest that the inhibitory neurotransmitter receptors, GluCls, are located in the neuropil containing the L1 or L2 neurons of the lamina or the α-processes of amacrine neurons.

Interestingly, MdGluCl immunostaining was also observed in the retina (Fig. 5B,C). The photoreceptor cells, retina basement membrane, and pigment cells were strongly immunoreactive. The L2 neurons are postsynaptic to the photoreceptor neurons R1-6, and the axon of L2 neurons forms feedback synapses on the photoreceptor terminals in the lamina of *Musca* and *Drosophila* (Kral and Meinertzhagen, 1989; Meinertzhagen and O'Neil, 1991). Although GluCls may be expressed in the photoreceptor cells, strong staining appears to be present in the pigment cells surrounding the pseudocone in the distal retina.

An immunopositive reaction with the anti-MdGluCl antibody was also observed in the thorax (Fig. 7A,B). The MdGluCl staining coincided with the motor neuron cell bodies clustered anterior and posterior to the thoracic neuropils (Baek and Mann, 2009;

Brierley et al., 2012), which were demonstrated to be glutamatergic using the vGluT-Gal4 driver in *Drosophila* (Baek and Mann, 2009). Glutamate elicited a hyperpolarizing response when applied to the cockroach fast coxal depressor motor neurons (Wafford and Sattelle, 1989). These findings suggest that the motor neurons receive and release glutamate. The anti-GluCl staining contrasts with punctuate staining by anti-MdRdl antibody in the neuropil of the thoracic ganglion (Fig. 7A,B,D,E). Punctuate labeling with a GABA antibody, which indicates GABAergic terminals, was observed in the thoracico-abdominal ganglion of *Drosophila* (Boerner and Duch, 2010). Further studies will be needed to examine the connection between this anti-GABA (presynaptic) staining and anti-MdRdl (postsynaptic) staining in the neuropil of the thoracic ganglion.

Longitudinal sections of the femur of the prothoracic leg showed intense striated staining with the anti-MdGluCl antibody (Fig. 7C). This is consistent with the high expression of the MdGluCl transcript in the leg (Fig. 4A). In electrophysiological characterization in *Xenopus* oocytes injected with mRNA isolated from the leg muscle (mainly containing metathoracic femoral muscles) of *S. gregaria*, hyperpolarizing receptors for glutamate were detected together with depolarizing receptors (Fraser et al., 1990). Given that hyperpolarizing responses to glutamate were also observed in the locust muscles (Cull-Candy and Usherwood, 1973), these findings suggest that GluCls might be expressed in the postsynaptic membrane of muscle fibers (Soler et al., 2004).
In contrast to GABACls, information on the distribution of GluCls in insects is limited. When the *Drosophila* GluCl cDNA was first cloned, multiple GluCl transcripts of different sizes were identified in the embryo, larvae, and adult (head) by northern blot analysis (Cully et al., 1996). Western blot analysis and *in situ* hybridization in the honeybee (*Apis mellifera*) brain indicated that the GluCl subunit is expressed in the antennae, antennal lobe, superior protocerebrum, optic lobe, and thoracic muscle (El Hassani, 2012). The honeybee GluCls were recently reported to be expressed in the glomeruli of the antennal lobe, the mushroom body, and the central complex rather than in the optic lobe (Démares et al., 2013). It was also shown that two splice variants are differentially expressed in the honeybee brain: one in the neuropils and one in the cell bodies. Related to the expression in the mushroom body, it was postulated that GluCls play a role in processes perceiving the conditioned stimulus in olfactory associative learning in the honeybee, whereas GABACls are involved in the consolidation of olfactory memory (Boumghar et al., 2012). It is surprising that the distribution pattern of MdGluCls was substantially different from that of honeybee GluCls. No intense MdGluCl immunolabeling was detected in the mushroom body, the

glomeruli of the antennal lobe, and the central body in the housefly. In these regions of fruit flies and houseflies, Rdl but not GluCl was highly expressed (Fig. 6B,C; Harrison et al., 1996). Recent studies revealed that DvGluT is expressed between glomeruli in *Drosophila*, whereas the vesicular GABA transporter is expressed within glomeruli (Liu and Wilson, 2013). GABACls and GluCls play distinct roles in olfactory processing in the antennal lobe.

In conclusion, our data show that two similar inhibitory neurotransmitter receptors, GluCls and GABACls, are differentially distributed in the housefly. GluCls are plentiful in the optic lobe and the leg motor neurons, whereas GABACls are more widely distributed in the brain. The two receptors might have different physiological roles in a variety of insect body parts. Further studies are needed to discern probable different physiological roles.

Chapter 3

Expression pattern and function of alternative splice variants of glutamate-gated chloride channel

Introduction

Glutamate is a major neurotransmitter in both vertebrates and invertebrates. Glutamate acts as an excitatory neurotransmitter in vertebrates, whereas it functions as both an excitatory and an inhibitory neurotransmitter in invertebrates. Two closely related amino acids, GABA and glutamate, play an important role as the major inhibitory neurotransmitters in invertebrates. Glutamatergic inhibitory neurotransmission is mediated by pentameric GluCls in the invertebrate nervous system. The cloning of the orthologous DNAs encoding GluCl subunits was described in several insect species (Cully et al., 1996; Eguchi et al., 2006; El Hassani et al., 2012; Janssen et al., 2007; Kwon et al., 2010).

GluCls, which belong to the family of Cys-loop receptors, are formed by five subunits arranged to form a chloride-permeable pore at the center (Jones and Sattelle, 2008; Ozoe, 2013). Each subunit has an extracellular N-terminal domain, which contributes to an orthosteric glutamate-binding site, and four transmembrane α-helices (M1-M4), which form a channel domain. Glutamate binding to the orthosteric site induces the opening of the channel to enhance the membrane permeability to chloride ions. Insect GluCls serve as a target of insecticides such as fipronil and avermectins (Kane et al., 2000; Kwon et al., 2010; Zhao et al., 2004b). A single subunit (α) is sufficient for the action of glutamate and avermectins in insects, whereas two subunits (α and β) are required for the action of both compounds in the nematode *Caenorhabditis elegans* (Cully et al., 1994, 1996). An X-ray crystallography study of a homomeric GluCl-α channel from *C. elegans* revealed the location of the binding sites for ligands, such as glutamate and ivermectin B_{1a} (Hibbs and Gouaux, 2011).

The tissue localization of GluCls has been previously studied in the honeybee (*Apis mellifera*) and the housefly (*Musca domestica*) (El Hassani et al., 2012; Kita et al., 2013). GluCls are predominantly located in the lamina of the optic lobe, leg motor neurons, and legs of the adult housefly, whereas GABACls are abundant in the

protocerebrum in addition to the medulla of the optic lobe (Kita et al., 2013), suggesting that the two inhibitory neurotransmitter receptors may play different physiological roles. The physiological roles of GluCls are now being unraveled; GluCls have recently been implicated in flight and waking control (Janssen et al., 2007), inhibitory actions on the olfactory system (Liu and Wilson, 2013), olfactory learning and memory (Boumghar et al., 2012; El Hassani et al., 2012), rest and arousal (McCarthy et al., 2011), and rhythmic light avoidance (Collins et al., 2012). The molecular functions and pharmacological properties of GluCls have also been investigated in both native and heterologously expressed forms; unique characteristics of insect GluCls have been revealed in terms of a lack of avermectin potentiation of glutamate currents in cloned *Drosophila* GluCls (Cully et al., 1996), a low sensitivity of cloned housefly GluCls to GABACl blockers (Eguchi et al., 2006), co-existence of two pharmacologically distinct GluCls in cockroach neurons (Raymond et al., 2000), and different sensitivities of desensitizing and non-desensitizing GluCls to GABACl blockers in cockroach neurons (Zhao et al., 2004a,b).

GluCls are diversified by the alternative splicing of their subunit gene (*GluCl*). It was reported that the *Drosophila GluCl* is spliced to generate two variants termed modules 1 and 2 (Semenov and Pak, 1999). Furthermore, the *Drosophila* genome database reveals that an additional variant arises from the alternative splicing of exon 3. Three GluCl subunit variants derived from the alternative splicing of exon 3 are present in the honeybee (Démares et al., 2013). However, little is known about the differences in the physiological roles and the pharmacological properties of GluCls containing different variants in any insect. Therefore, I investigate the presence of *GluCl* variants in the housefly, the transcript expression levels in the different body parts and different stages of the housefly, and the functional and pharmacological differences between MdGluCls formed by variants expressed in *Xenopus* oocytes. In this chapter, I describe in this chapter that the variants are differentially expressed in the body parts and that functionally indistinguishable but pharmacologically distinct channels are formed by the splice variants.

Materials and methods

Chemicals

[^{3}H]Ivermectin B_{1a} (50 Ci/mmol) and unlabeled ivermectin B_{1a} were purchased from American Radiolabeled Chemicals Inc. (St. Louis, MO) and Sigma-Aldrich (St.

Louis, MO), respectively. Sodium hydrogen L(+)-glutamate monohydrate, fipronil, and PTX were purchased from Wako Pure Chemical Industries, Ltd. (Osaka, Japan).

Animals

The WHO/SRS strain of houseflies (*Musca domestica* L.) was used throughout the experiments. The larvae were reared on a wet medium containing a bran and powder diet CE2 (Clea Japan, Tokyo, Japan) at 25 °C, and the adults were supplied with water and sugar. Mature female African clawed frogs (*Xenopus laevis*) were purchased from Shimizu Laboratory Supplies Co., Ltd. (Kyoto, Japan).

RNA isolation and cDNA synthesis

The heads, thoraces, abdomens, and legs of adult male houseflies (2-3 days after eclosion), the head parts of pupae (1 day after pupation), and the head parts of larvae (3-4 days after hatching) were excised using scissors. Total RNA was isolated from these parts and from embryos using Isogen® (Wako Pure Chemical Industries, Ltd.). The thorax samples did not contain legs or wings. Total RNA (1 μg) was run on a 1% formaldehyde-agarose gel to determine the RNA quality. First-strand cDNA was synthesized from the gDNA Eraser-treated total RNA (1 μg) by priming with oligo-dT primers and random 6-mers using the PrimeScript® RT Reagent Kit with gDNA Eraser (Takara Bio Inc., Shiga, Japan) according to the manufacturer's instructions.

Cloning of MdGluCl splice variants

The cloning of *MdGluClA* (DDBJ accession No. AB177546) was previously reported as *MdGluCl-α* (Eguchi et al., 2006). An *MdGluClB* fragment containing exon 3 was obtained by PCR using KOD -Plus- (Toyobo Co. Ltd., Osaka, Japan), the oligonucleotide primers, MdG-25bF (5'-CAAACACATAACGCGCAGC-3') and MdG-261R (5'-CAATTACCAGCATACAGCATGGG-3'), and cDNA prepared from the heads of male adult houseflies as a template. A fragment located downstream of exon 3 was amplified by PCR using MdG-223RF (5'-AACAGTAAAACCAACACGG-3'), MdG-1398bR (5'-CGTCATCATCATCAATGGTC-3'), and pcDNA3-*MdGluClA* as a template. Full-length *MdGluClB* (DDBJ accession No. AB698079) was amplified by PCR using the two fragments as a template. An *MdGluClC* fragment containing exon 3 was

obtained by PCR using the primers, MdG3-59F (5’-GATAATAAGGCCACCAATG-3’) and MdG-177GR (5’-TGGCCATACGTAGTGAAC-3’). MdG3-59F was designed based on the DNA sequence of *Drosophila* GluCl-α variant C (GenBank accession No. NM_001014641). An *MdGluClC* fragment was amplified using MdG-25bF and MdG3-79R (5’-CATCGATTTTTGAAATTGAC-3’), and another fragment was amplified using MdG3C-60RF (5’-AACTTACCCACCTATGTCTACG-3’) and MdG-1398bR. Full-length *MdGluClC* (DDBJ accession No. AB698080) was amplified by PCR using the two fragments. Finally, the *Kpn*I and *Xba*I sites were attached to full-length *MdGluCl*s by PCR using the primers MdG-KpnIF (5’-TTGGTACCGAGCTATGGGAACCGGTCATTT-3’) and MdG-XbaIR (5’-TAGGGCCCTTAGAAAGTCTCATCCTC-3’). The amplified full-length cDNAs of *MdGluCl* variants were inserted into the pTA2 vector to confirm their sequences. After the confirmation, these *MdGluCl* variants were inserted into the *Kpn*I and *Xba*I sites of the pcDNA3 vector (Invitrogen, Carlsbad, CA).

Isolation of genomic DNA

An extraction buffer (1 M Tris-HCl, 0.5 M EDTA, 5.6 M NaCl, 10% SDS, pH 7.6) was maintained at 60 °C. An adult housefly (3-5 days after eclosion) was homogenized in the presence of liquid nitrogen. The homogenate was added to the extraction buffer. After incubation for 30 min at room temperature, the homogenate was centrifuged for 90 s at 15,000 ×*g*. To the supernatant were added a one-tenth volume of 3 M sodium acetate and a 2-fold volume of ethanol. The solution was cooled at -20 °C and then centrifuged for 5 min at 15,000 ×*g*. The supernatant was removed, and the pellet was rinsed twice with 70% ethanol. The pellet was suspended in 70% ethanol and centrifuged for 5 min at 15,000 ×*g*. The supernatant was removed, and the pellet was dried. Finally, the pellet was dissolved in TE buffer (10 mM Tris-HCl, 1 mM EDTA, pH 8.0).

Quantitative PCR (qPCR)

qPCR was performed using cDNA prepared from 10 ng of total RNA, the THUNDERBIRD™ SYBR® qPCR Mix (Toyobo Co., Ltd.), and gene specific primers in a Thermal Cycler Dice® Real Time System (Takara Bio Inc.). The gene-specific primers, MdG-19F (5’-GCATCACTAGCTAATAATGCC-3’) and MdG3A-68RR (5’-CAGATTGATTCTGACTATGGC-3’), MdG2-74F

(5’-CAAAAATCGATGATGTTACC-3’) and MdG-118GR (5’-AACAAATCAGGCATCCAG-3’), and MdG3C-60RF and MdG-97R (5’-ACGTTCATCTGTCCATTG-3’), were used to amplify *MdGluClA*, *B*, and *C*, respectively. All the procedures were conducted according to the manufacturer’s instructions. The PCR program consisted of 95 °C for 30 s for initiation, 40 cycles of 95 °C for 5 s and 58 °C for 30 s, followed by 95 °C for 15 s, 58 °C for 30 s and 95 °C for 15 s for the dissociation curve analysis. The specific amplification was assessed by the electrophoresis of the PCR products on a 4% agarose gel and melting curve analysis. Standard curves were constructed using eight serial 4-fold dilutions of synthesized cDNA starting with 100 ng per reaction. This analysis was replicated three times using independent samples. The expression levels of three types of *MdGluCl* variants were normalized using ribosomal protein subunit 3 (*RpS3*) as an internal control. The primers Md-RPS3_F (5’-AAGCTGAATCTCTCCGTTAC-3’) and Md-RPS3_R (5’-GACGACGACTTCACAGC-3’) were used to amplify the housefly *RpS3* gene (DDBJ accession No. AF207603).

cRNA preparation and injection into Xenopus oocytes

Three *MdGluCl* variants were amplified by PCR using KOD -Plus- NEO (Toyobo Co., Ltd.), pcDNA3-*MdGluClA*, -*MdGluClB*, or -*MdGluClC* as templates, and the primers pcDNA3-cRNAF (5’-CTCTCTGGCTAACTAGAGAACC-3’) and pcDNA3-cRNAR (5’-AACTAGAAGGCACAGTCGAG-3’). The PCR products were purified using the illustra™ GFX™ PCR DNA and Gel Band Purification Kit (GE Healthcare UK, Ltd., Little Chalfont, UK), and their DNA sequences were confirmed. The capped RNAs were synthesized by T7 polymerase, using the mMESSAGE mMACHINE® T7 Ultra Kit (Ambion, Austin, TX) and 100 ng of purified PCR products. The quality and quantity of synthesized cRNAs were assessed by agarose gel electrophoresis and absorption spectroscopy. The synthesized cRNAs were stored at -20 °C until use.

Mature female *X. laevis* was anesthetized with 0.1% (w/v) ethyl *m*-aminobenzoate methanesulfonate (Wako Pure Chemical Industries, Ltd.), and the ovarian lobes were dissected out. The ovarian lobes were treated with collagenase (2 mg/ml; Sigma-Aldrich) in Ca^{2+}-free standard oocyte solution (SOS) (100 mM NaCl, 2 mM KCl, 1 mM $MgCl_2$, 5 mM HEPES, pH 7.6) for 60-120 min at room temperature. After the treatment, the oocytes were gently washed with SOS (100 mM NaCl, 2 mM KCl, 1 mM $MgCl_2$, 1.8 mM $CaCl_2$, 5 mM HEPES, pH 7.6) containing 2.5 mM sodium

pyruvate, gentamycin (50 μg/ml; Gibco, Langley, OK), penicillin (100 U/ml; Invitrogen) and streptomycin (100 μg/ml; Invitrogen), and they were incubated in the same buffer at 16 °C overnight. The oocytes were injected with 5 ng (for [^{3}H]ivermectin B_{1a} binding assay and Western blotting) or 30 ng of each cRNA (for analysis of channel functions) and incubated under the same conditions for one to three days. Alternatively, the oocytes were co-injected with a total of 30 ng of cRNAs of different variants in the following ratio: *MdGluClA*:*B* = 1:1; *MdGluClA*:*C* = 3:1; *MdGluClB*:*C* = 3:1; and *MdGluClA*:*B*:*C* = 3:3:1).

Preparation of membranes from Xenopus oocytes

Fifty *Xenopus* oocytes that responded to 100 μM glutamate with 0.5-1 μA of induced current were chosen and homogenized in homogenization buffer (HB; 250 mM sucrose, 10 mM HEPES, 1 mM EGTA, and, 2 mM $MgCl_2$, pH 7.6) using a Teflon-glass homogenizer. The homogenates were centrifuged for 5 min at 500 ×*g*. The supernatants were centrifuged for 30 min at 25,000 ×*g*. The supernatants were removed, and the pellets were washed superficially with HB. The pellets were then suspended in HB and centrifuged for 30 min at 25,000 ×*g*. The pellets were washed again to remove yolk granules, suspended in HB, and centrifuged for 30 min at 25,000 ×*g* again. The pellets were resuspended in 50 mM HEPES buffer (pH 7.4) and used for the [^{3}H]ivermectin B_{1a} binding assay after protein quantification by the Bradford method (Bradford, 1976).

[^{3}H]Ivermectin B_{1a} binding experiments

A mixture of dimethyl sulfoxide (DMSO) (4 μl), 1 nM [^{3}H]ivermectin B_{1a}, and oocyte membranes (20 μg protein) was incubated for 60 min at 22 °C in 0.5 ml of 50 mM HEPES buffer containing 0.02% Triton X™-100 (pH 7.4) for determination of the total binding. For determination of nonspecific binding, DMSO (4 μl) containing 125 μM ivermectin B_{1a} was added instead of DMSO alone. As a negative control, membranes prepared from oocytes injected with nuclease-free water instead of variant cRNAs were used. After the incubation, the mixtures were filtered through Whatman GF/B filters and washed twice with 5 ml of 10 °C-cold water containing 0.1% Triton X-100™ using a Brandel M-24 cell harvester. The filters were pre-immersed in 50 mM HEPES buffer containing 0.1% polyethylenimine (pH 7.4). The radioactivity on the filter was counted in a toluene/2-methoxyethanol-based scintillation fluid using a

Beckman LS 6000 SE liquid scintillation spectrometer. Specific binding (dpm) was obtained by subtracting nonspecific binding (dpm) from total binding (dpm). Each experiment was performed in triplicate and repeated three times.

Western blotting.

The oocyte membranes were suspended in the Laemmli buffer (50 mM Tris-HCl, 10% glycerol, 2% SDS, 5% β-mercaptoethanol, 0.02% bromophenol blue, pH 6.8). After being boiled for 5 min at 96 °C, the membrane proteins were loaded onto a 7.5% sodium dodecyl sulfate (SDS)-polyacrylamide gel with a 5% stacking gel. After SDS-polyacrylamide gel electrophoresis, the proteins were transferred to a PVDF membrane (Immobilon™-P; Merck Millipore, Billerica, MA). The PVDF membrane was incubated in phosphate-buffered saline with 0.1% Tween™ 20 (PBST) containing 5% dried milk (blocking buffer) for 1 h at room temperature. After the blocking, the PVDF membrane was incubated with a purified anti-MdGluCl antibody (Kita et al., 2013) or anti-beta Actin antibody (mAbcam 8224) - Loading Control (Abcam, Cambridge, UK) at a dilution of 1:1000 with a blocking buffer for 2 h at 37 °C. After the incubation, the membrane was washed with PBST four times and incubated with a stabilized peroxidase-conjugated goat anti-rabbit or anti-mouse IgG (H+L) (1 μg/ml; Thermo Fisher Scientific Inc., Waltham, MA) that was diluted at 1:500 with a blocking buffer for 1 h at 37 °C. The immunoreactivity was detected with SuperSignal® West Femto Maximum Sensitivity Substrate (Thermo Fisher Scientific Inc.) using ImageQuant™ LAS 4000 (GE Healthcare UK, Ltd.).

Two-electrode voltage-clamp recordings

The glutamate-induced currents were recorded by a two-electrode voltage-clamp (TEVC) method using an Oocyte Clamp OC-725C amplifier (Warner Instruments, Hamden, CT). The oocytes were kept in SOS and clamped at a membrane potential of -80 mV. The glass capillary electrodes were filled with 2 M KCl and had a resistance of 0.5-1.5 MΩ. The recorded currents were analyzed using Data-Trax2™ software (World Precision Instruments Inc., Sarasota, FL). The experiments were performed at 18-22 °C. Glutamate was dissolved in SOS and applied to the oocytes for 3 s. After the glutamate application, the oocytes were washed by SOS for more than 30 s and assessed for their integrity. Ivermectin B_{1a} was first dissolved in DMSO and then diluted with SOS. The ivermectin B_{1a} solution containing 0.1% DMSO was applied to

oocytes for 20 s, and the oocytes were then washed with SOS for 3 min. The chloride channel blockers were first dissolved in DMSO and then diluted with SOS. Glutamate at 10 μM was first applied to oocytes several times to get a control response. The blocker solution containing 0.1% DMSO was perfused for 3-10 min until a stable inhibition of the glutamate response was reached. The inhibition percentage was calculated from the average of two minimum responses to 10 μM glutamate during the perfusion of a blocker. Fifty percent effective concentrations (EC_{50}s), Hill coefficients (n_Hs), and fifty percent inhibitory concentrations (IC_{50}s) were obtained from concentration-response relationships by nonlinear regression analysis using OriginPro 8J (Origin Lab, Northampton, MA). These values are presented as mean ± SEM. Data were obtained for at least six oocytes from at least two frogs.

Statistics

Data are presented as the mean ± SEM determined from at least three separate experiments. Significance was analyzed using unpaired Student's *t*-test.

Results

Cloning of MdGluCl splice variants and identification of RNA editing sites

Full-length *MdGluCl*s that have different sequences at exon 3, designated as A, B, and C, were obtained by PCR. Exons 3A and 3B are composed of 68 nucleotides, and exon 3C has 71 nucleotides (Fig. 8A). The three exons share nucleotide and amino acid identities of 39.4% and 41.7%, respectively. *MdGluCl*s contain RNA editing sites in addition to alternatively spliced exons (Fig. 8B). I examined the nucleotide sequences of 42 clones of *MdGluClA*, 4 clones of *MdGluClB*, and 5 clones of *MdGluClC* in the plasmid vector. Four nucleotides (78, 79, 526 [529], and 722 [725]) in the cloned *MdGluCl*s had two variations, A and G (Fig. 8B), and the corresponding nucleotides in the genomic DNA were all A (Note that the numbers in brackets are for *MdGluClC*). Three of these changes alter amino acid residues (Fig. 8B). A79 in *MdGluClA*, G78 and A722 in *MdGluClB*, and G529 in *MdGluClC* were not found in the sequenced clones of each variant (Table 1). *MdGluClA*, *B*, and *C* that contain A78, G79, A526 [529], and A722 [725] were used for the subsequent studies. This combination of editing was chosen as this was a predominant combination (21%) found in *MdGluClA*, a major splice variant (Table 2). I aimed to investigate the effects of alternative splicing

on agonist and blocker potencies, using splice variants with a fixed editing pattern. Figure 8C schematically represents the positions corresponding to exon 3 and RNA editing sites in the MdGluCl subunit.

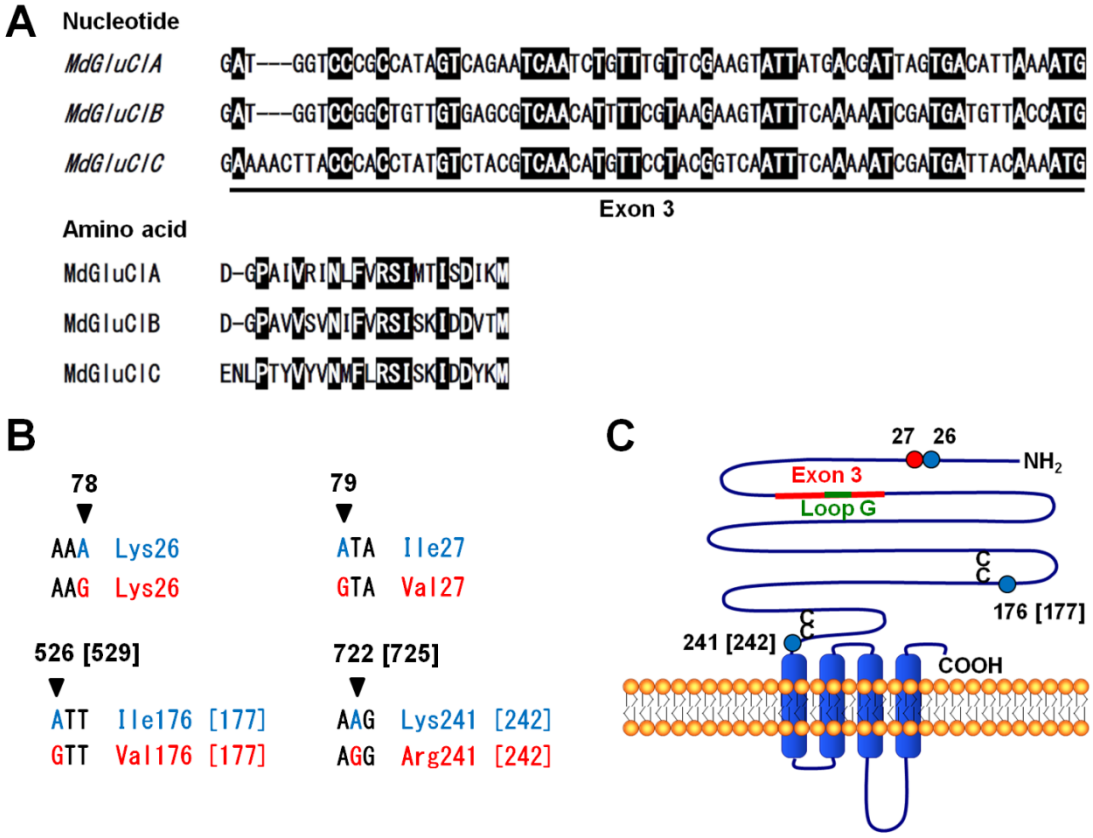

Fig. 8. Alternative splicing and RNA editing of *MdGluCl*.

(A) Nucleotide and deduced amino acid sequences of three *MdGluCl* splice variants. Fully conserved nucleotides and amino acids are shaded in black. (B) RNA editing of *MdGluCl*. Note that the numbers in brackets are for *MdGluClC* or MdGluClC. (C) The positions of alternatively spliced exon3 and RNA editing sites schematically indicated on the MdGluCl subunit. Note that the numbers in brackets are for *MdGluClC* or MdGluClC.

Table 1

Site-specific RNA editing found in *MdGluCl* clones

Variant	RNA editing site								n[b]
	78		79		526 [529][a]		722 [725]		
	A	G	A	G	A	G	A	G	
	AA**A**[c]: Lys	AA**G:** Lys	**A**TA: Ile	**G**TA: Val	**A**TT: Ile	**G**TT: Val	AA**A**G: Lys	A**G**G: Arg	
MdGluClA	21	21	0	42	32	10	20	22	42
MdGluClB	4	0	1	3	2	2	0	4	4
MdGluClC	4	1	1	4	5	0	4	1	5

[a]Nucleotide numbers in brackets are for *MdGluClC*.

[b]*n*: number of clones analyzed.

[c]Bold characters represent RNA editing sites in codons.

Table 2

Combinations of RNA editing found in *MdGluCl* clones

Variant	RNA editing pattern at nucleotide positions 78, 79, 526 [529], and 722 [725][a]									n[b]
	A,A,A,G	A,G,A,A	A,G,A,G	A,G,G,A	A,G,G,G	G,G,A,A	G,G,A,G	G,G,G,A	G,G,G,G	
MdGluClA	0	**9**[c]	8	1	3	7	8	3	3	42
MdGluClB	1	0	1	0	**2**	0	0	0	0	4
MdGluClC	1	**3**	0	0	0	1	0	0	0	5

[a]Nucleotide numbers in brackets are for *MdGluClC*.

[b]*n*: number of clones analyzed.

[c]Bold characters represent the most prevalent combination in each variant.

Expression patterns of three splice variants in the housefly

I next investigated the expression of the transcripts of three splice variants in the different body parts of the adult housefly and different developmental stages by qPCR (Fig. 9). *MdGluClA* and *B* were predominantly expressed in the adult head (Fig. 9A). *MdGluClC* was expressed not only in the adult head but also in the thorax, legs, and abdomen. In the adult legs and abdomen, *MdGluClC* showed high expression levels compared with the other variants. All variant transcripts were abundant in the adult head compared with the pupal head, the larval head, and the whole embryo. In the larval stage, *MdGluClB* was significantly highly expressed compared with other variant transcripts (p <0.05) (Fig. 9B).

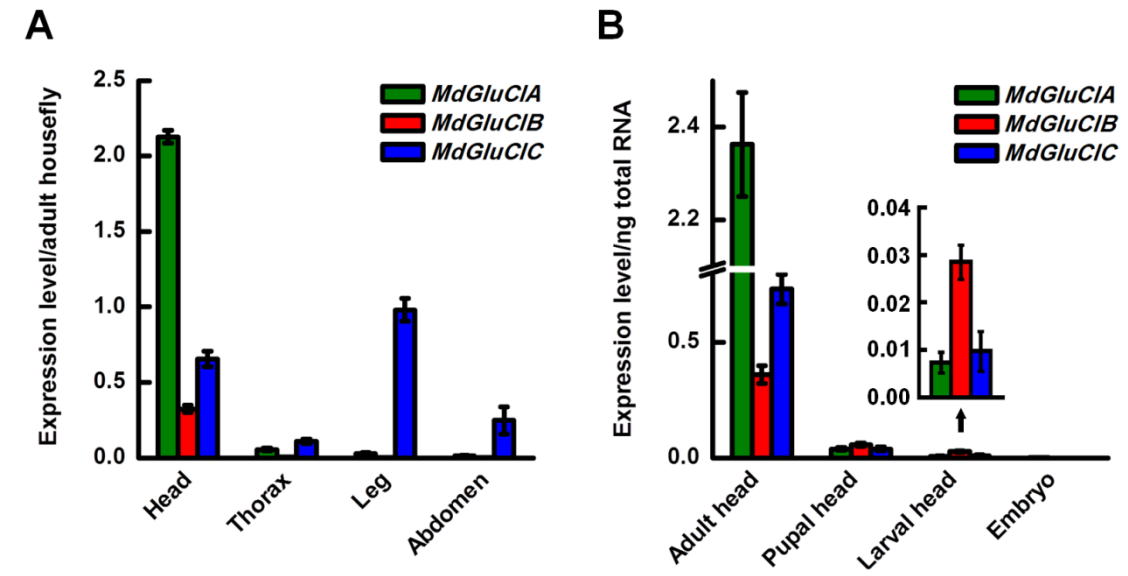

Fig. 9. Expression patterns of the transcripts of three *MdGluCl* variants in the housefly.

(A) Expression levels of *MdGluCl* variants in the adult body parts. The data indicate relative expression levels per adult housefly. (B) Expression levels of *MdGluCl* variants in the developmental stages. The data indicate relative expression levels per ng of total RNA. The results are normalized relative to the internal control *RpS3*. The data are the means ± SEM (n=3).

Expression efficiencies of three variants in oocyte membranes

I performed TEVC experiments to investigate whether there are functional differences between MdGluCls formed by different variants expressed in *Xenopus* oocytes. Prior to the functional analysis, I examined the expression efficiencies of three

variants in oocyte membranes using binding assays with the high-affinity GluCl ligand [^{3}H]ivermectin B_{1a} and Western blotting (Fig. 10). Specific binding constituted ≈100% of total binding. The highest levels of specific [^{3}H]ivermectin B_{1a} binding were obtained in the membranes of oocytes injected with MdGluClC cRNA, when compared using the same amount of membrane protein (Fig. 10A). The level of specific [^{3}H]ivermectin B_{1a} binding to MdGluClC channels was approximately 3-fold higher than that to MdGluClA or B channels, although there was no significant difference in the levels of specific binding to a membrane protein between MdGluClA and B channels. Consistent with the result from the [^{3}H]ivermectin B_{1a} binding assays, the intensity of the anti-MdGluCl antibody-reactive band at approximately 52 kDa on the Western blot was higher for the MdGluClC subunit than for the MdGluClA or B subunit (Fig. 10B). Based on these results, 3-fold less MdGluClC cRNA was injected than MdGluClA and B cRNA in the co-injection experiments.

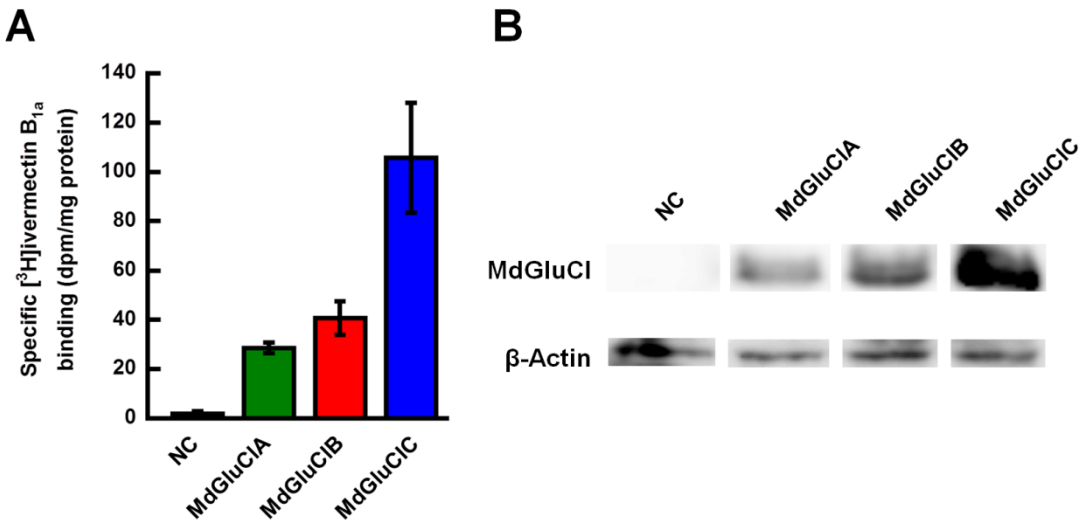

Fig. 10. Expression of MdGluCl channels containing different variant subunits in *Xenopus* oocytes.

(A) Expression levels of MdGluCls determined by [^{3}H]ivermectin B_{1a} binding to oocyte membranes. The data are the means ± SEM (n=3). (B) Western blot of the MdGluCl subunits in oocyte membranes with a specific antibody. The MdGluCl subunits were detected as a band of approximately 52 kDa. The internal control β-actin was detected as a band of approximately 43 kDa. As a negative control (NC), membranes prepared from oocytes injected with nuclease-free water instead of variant cRNAs were used.

Responses of channels containing different variants to glutamate

The glutamate responses of homomers formed by variants expressed in *Xenopus* oocytes were examined by the TEVC technique. The application of glutamate to all channels induced robust inward currents in a concentration-dependent fashion (Fig. 11A). The concentration-response curves gave EC_{50}s of 6.38 ± 0.80 μM, 9.11 ± 0.68 μM, and 7.25 ± 0.66 μM for MdGluClA, B, and C channels, respectively, and they produced n_Hs of 2.26 ± 0.22, 2.04 ± 0.14, and 1.78 ± 0.13 for MdGluClA, B, and C channels, respectively (Fig. 11B). No significant differences were observed in the EC_{50}s and n_Hs between the three MdGluCls expressed as homomers in oocytes (p >0.05).

As different variants may be co-assembled to form heteromeric GluCls in the housefly body, I examined the glutamate responses of MdGluCls containing different variants co-expressed in oocytes. The glutamate EC_{50}s for MdGluCls in oocytes co-injected with two or three variant cRNAs, A + B, A + C, B + C, and A + B + C, were 7.44 ± 0.87 μM, 6.40 ± 0.69 μM, 7.30 ± 0.64 μM, and 6.29 ± 0.34 μM, respectively, and the n_Hs were 3.02 ± 0.32, 3.13 ± 0.23, 3.24 ± 0.21, and 3.15 ± 0.13, respectively (Fig. 11C). No significant differences were observed in the EC_{50}s and n_Hs between oocytes co-injected with different MdGluCl variant cRNAs (p >0.05). There were significant differences in the n_Hs between oocytes that were singly and co-injected with MdGluCl variant cRNA(s) (p <0.05), whereas there were no differences in the EC_{50}s between these oocytes (p >0.05), suggesting that co-injection of different variant cRNAs yielded similar functional heteromeric channels on the oocyte membrane surface.

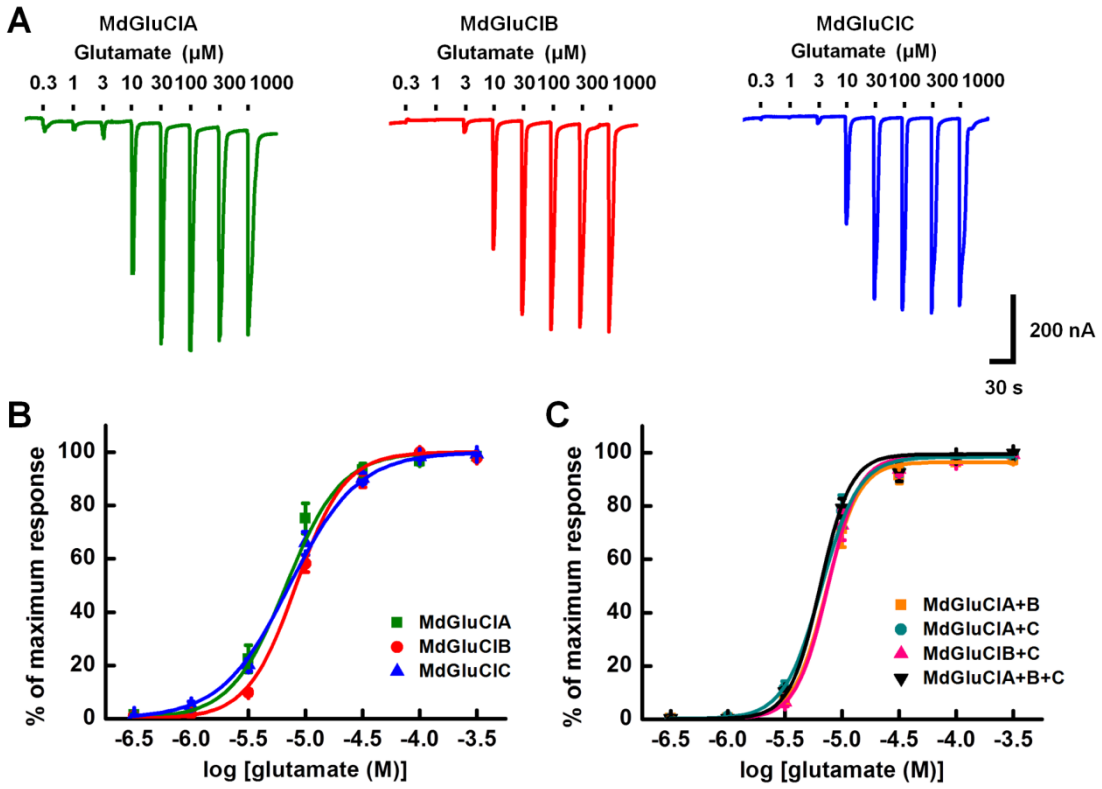

Fig. 11. Glutamate responses of MdGluCls containing variant subunits singly or co-expressed in *Xenopus* oocytes.

(A) Traces of currents induced by glutamate in channels containing singly expressed variants. (B) Glutamate concentration-response curves in channels containing singly expressed variants. (C) Glutamate concentration-response curves in channels containing co-expressed variants. The data are the means ± SEM (n=7-8).

Actions of ivermectin B_{1a} and chloride channel blockers

To examine whether alternative splicing causes differences in the pharmacological properties of MdGluCls, I tested an allosteric activator, ivermectin B_{1a}, and two representative blockers of ligand-gated chloride channels, PTX and fipronil. Applications of ivermectin B_{1a} induced irreversible currents (current traces not shown). Ivermectin B_{1a}-induced currents were observed in all channels in a dose-dependent manner (Fig. 12). There was no significant difference between the amplitudes of the currents induced by the same concentration of ivermectin B_{1a} in oocytes singly (Fig. 12A) and co-injected (Fig. 12B) with variant cRNA(s).

PTX and fipronil inhibited glutamate-induced currents in both homomeric and heteromeric channels (Figs. 13A, 14A). The IC_{50}s of PTX calculated from the

concentration-response relationships of MdGluClA, B, and C channels were 67.1 ± 8.6 μM, 63.2 ± 12.5 μM, and 255 ± 47 μM, respectively (Fig. 13B). MdGluClC channels were less sensitive to PTX than MdGluClA and B channels (p <0.01). The IC_{50}s of PTX in oocytes co-injected with different combinations of variant cRNAs, A + B, A + C, B + C, and A + B + C, were 32.1 ± 1.2 μM, 40.1 ± 3.3 μM, 33.2 ± 2.6 μM, and 32.5 ± 4.2 μM (Fig. 13C). There were no significant differences in PTX sensitivity between any combinations of variant subunits (p >0.05). However, the potencies of PTX were significantly increased by the co-expression of variants (p <0.05).

The dose-response curves of fipronil for MdGluClA, B, and C channels gave IC_{50}s of 746 ± 214 nM, 573 ± 107 nM, and 2.93 ± 0.67 μM, respectively (Fig. 14B). MdGluClC channels were significantly less sensitive to fipronil than MdGluClA (p <0.05) and B (p <0.01) channels. The IC_{50}s of fipronil for MdGluCls composed of two or three subunit variants, A + B, A + C, B + C, and A + B + C, were 537 ± 41 nM, 507 ± 78 nM, 499 ± 33 nM, and 659 ± 86 nM, respectively (Fig. 14C). The inhibitory potencies of fipronil did not differ between all channels formed by the combinations of variant subunits (p >0.05). However, the potencies of fipronil in the heteromeric expression were significantly high compared with homomeric MdGluClC expression (p <0.01).

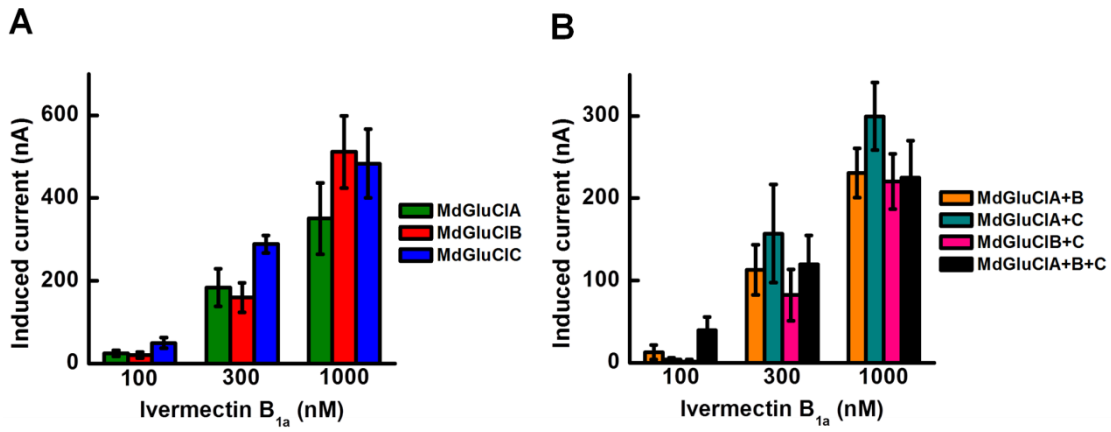

Fig. 12. Ivermectin B_{1a} responses of MdGluCls containing variant subunits singly or co-expressed in *Xenopus* oocytes.

(A) Maximum amplitude of ivermectin B_{1a}-induced currents in channels containing singly expressed variants. (B) Maximum amplitude of ivermectin B_{1a}-induced currents in channels containing co-expressed variants. The data are the means ± SEM (n=6).

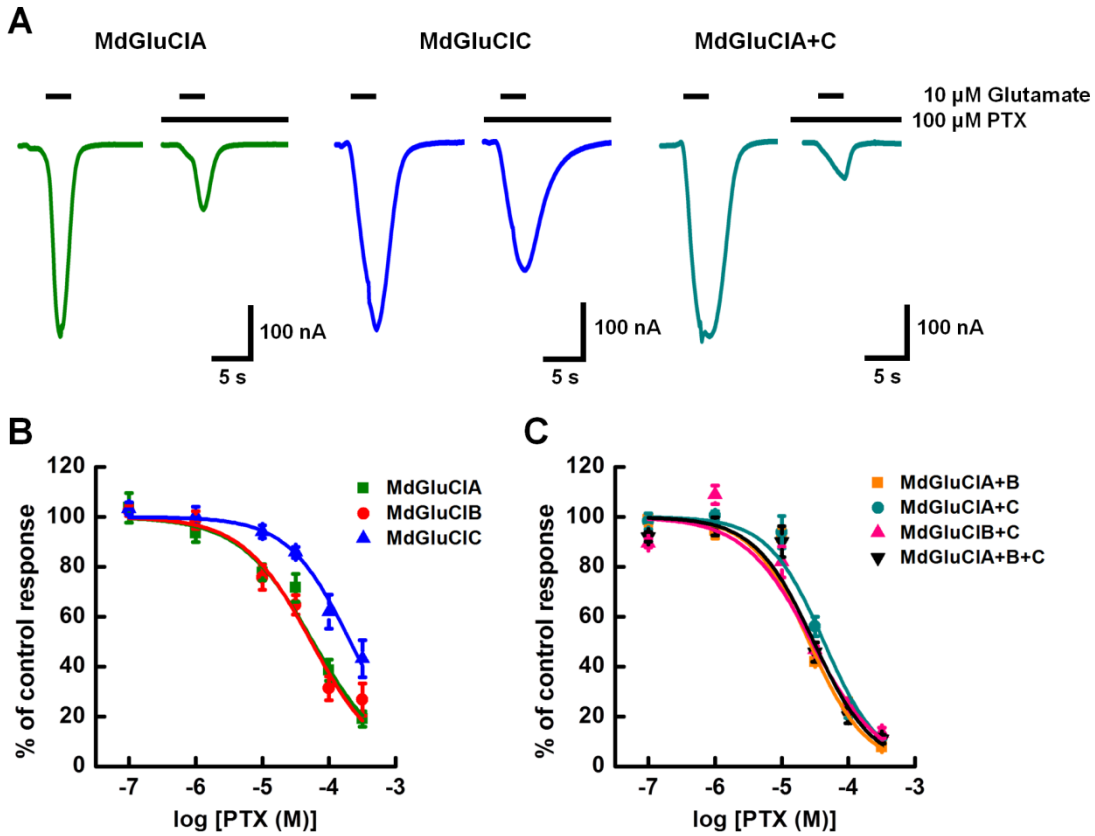

Fig. 13. PTX inhibition of glutamate-induced currents in MdGluCls containing variant subunits singly or co-expressed in *Xenopus* oocytes.

(A) Examples of PTX inhibition of currents in channels containing singly and co-expressed variants. (B) PTX concentration-response curves in channels containing singly expressed variants. (C) PTX concentration-response curves in channels containing co-expressed variants. The data are the means ± SEM (n=6).

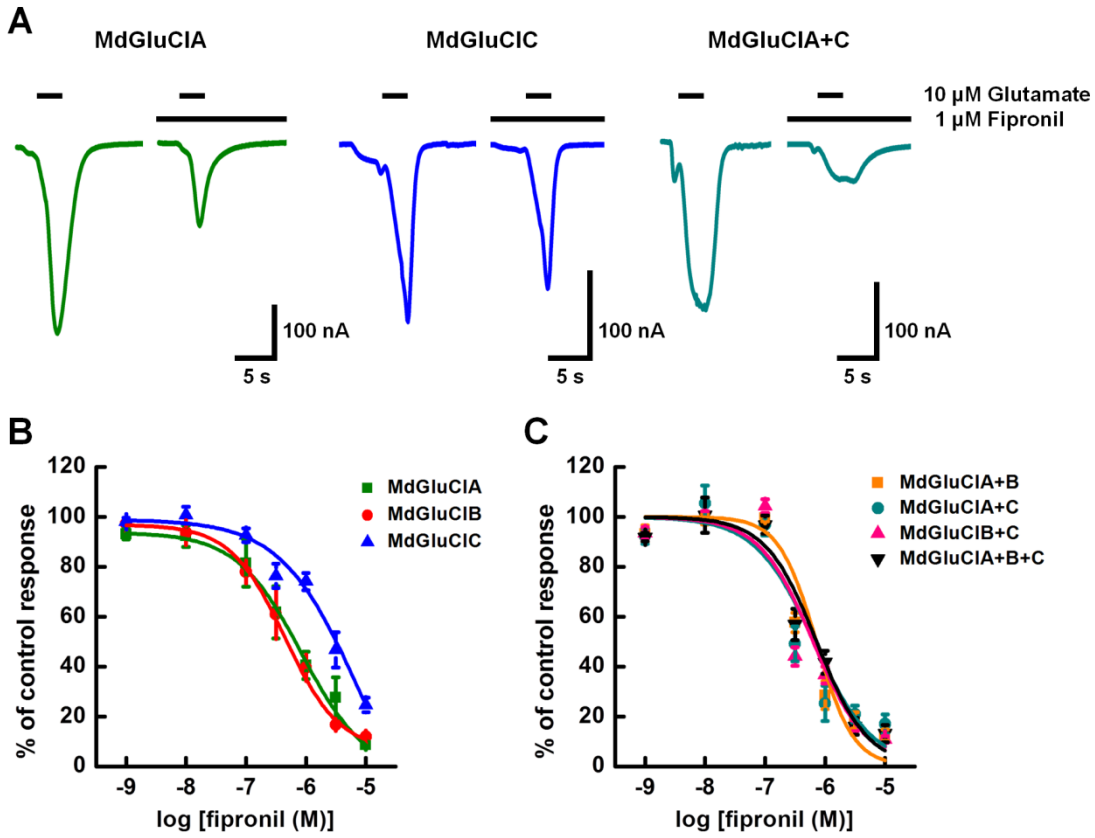

Fig. 14. Fipronil inhibition of glutamate-induced currents in MdGluCls containing variant subunits singly or co-expressed in *Xenopus* oocytes.

(A) Examples of fipronil inhibition of currents in channels containing singly and co-expressed variants. (B) Fipronil concentration-response curves in channels containing singly expressed variants. (C) Fipronil concentration-response curves in channels containing co-expressed variants. The data are the means ± SEM (n=6).

Discussion

Many neuronal proteins are diversified by pre-mRNA splicing, which produces distinct mRNAs from a single gene and then gives rise to variant proteins (Kornblihtt et al., 2013; Li et al., 2007). In the present study, I set out to examine the diversification of GluCls by alternative splicing in the housefly. I previously cloned the cDNA encoding the MdGluClA subunit from houseflies to examine the functional properties of MdGluCls (Eguchi et al., 2006). Here I describe the cloning of cDNAs encoding two additional MdGluCl subunit splice variants, MdGluClB and C (Fig. 8A). Although variants with amino acid identities of 100%, 95.7%, and 79.2% to variants A, B, and C,

respectively, have been identified in the genome sequence of *D. melanogaster*, functional and physiological analyses have not been performed to date. Three variants (Amel_Glu A-C) were recently identified from the honeybee *A. mellifera* (Démares et al., 2013). MdGluClA and B have amino acid identities of 91.3% and 95.7% to Amel_GluCl B (GenBank accession No. DQ667185.1) and Amel_GluCl A (GenBank accession No. NM_001077809.1), respectively. MdGluClC does not correspond to Amel_GluCl C. I also identified four pre-mRNA editing sites in *MdGluCl* in the present study (Fig. 8B). The pre-mRNA editing alters individual nucleotides by the action of adenosine deaminases that act on RNA (ADARs) (Jepson and Reenan, 2007; Keegan et al., 2001). Two nucleotide variations, A or G, were found at the nucleotide positions of 78, 79, 526 [529], and 722 [725] in the sequences of cloned *MdGluCls* (Note that the numbers in brackets are for *MdGluClC* or MdGluClC). In the *Musca* genomic DNA sequences, the nucleotides at all the four positions were found to be A, indicating that these variations arises from A-to-I pre-mRNA editing. Of the four sites, three equivalents (78, 79, and 722 [725]) are found in *Drosophila* GluCl-α, in which five editing sites were identified (Semenov and Pak, 1999). Changes at positions 79, 526 [529], and 722 [725] lead to the amino acid changes of Ile27 to Val27, Ile176 [177] to Val176 [177], and Lys241 [242] to Arg241 [242], respectively. These findings indicate that MdGluCls are diversified by RNA splicing and editing.

To gain the basis to understand the physiological roles of MdGluCls containing different subunit variants, I examined the expression patterns of the variants using qPCR analysis. The results showed that *MdGluClA* and *B* are abundantly expressed in the head of the adult housefly, whereas *MdGluClC* is expressed in the head, thorax, legs, and abdomen (Fig. 9A). Our previous immunohistochemical study using an anti-MdGluCl antibody has shown that intense staining was detected in the femur of the leg. The present findings suggest that the GluCls expressed in the legs and abdomen is the variant-C homo-pentamer because the variant C transcript is exclusively enriched in these tissues. The variant most highly expressed in the adult head was *MdGluClA*, followed by *MdGluClC*. It is tempting to speculate that native channels in the adult head may be heteromeric assemblies of different variants, although more experiments are needed to draw a solid conclusion. All three splice variants are highly expressed in the adult stage compared with immature developmental stages (Fig. 9B). Although the expression levels of *MdGluCls* in the larval head are relatively low compared with that of the adult head, *MdGluClB* was significantly more abundant than *MdGluClA* and *C* in the larval head. These findings suggest that the predominant variants are changed after metamorphosis.

I next investigated the glutamate sensitivity of channels formed by singly or co-injecting variant cRNA(s) into *Xenopus* oocytes. The application of glutamate to all the channels expressed in oocytes induced robust inward currents in a concentration-dependent fashion (Fig. 11A). When a single variant cRNA was injected, there was no significant difference in the EC_{50}s and n_Hs between homomeric channels expressing three variants (Fig. 11B). As there is a possibility that heteromeric channels containing different variants are expressed in the head, in which the transcripts of three variants were detected, I examined the glutamate sensitivity of oocytes co-injected with two or three different variant cRNAs. The coefficient n_Hs (≈3) in oocytes co-injected with RNAs differed from n_Hs (≈2) in singly-injected oocytes, suggesting that positive cooperativity among multiple binding sites was changed by the formation of heteromeric channels. However, there were no differences in the EC_{50}s and n_Hs between channels formed by any combinations of variants. These findings indicate that the alternative splicing of exon 3 does not affect glutamate sensitivity. An X-ray crystallography study of the *C. elegans* GluCl-α channel revealed that the orthosteric site is formed by loop A-G in the N-terminal extracellular domain (Hibbs and Gouaux, 2011). Exon 3 encompasses loop G, in which Arg37 [38] forms an electrostatic interaction with the α-carboxylate of glutamate (Note that the number in the bracket is for MdGluClC). The equivalent Arg is conserved in all three MdGluCl variants. This could explain why the substitution of exon 3 by alternative splicing does not affect glutamate sensitivity. This is in contrast to the case with GABACls. The *Drosophila* GABACl subunit gene *Rdl* also undergoes pre-mRNA splicing and editing. The changes by these processes cause differences in the sensitivity of the receptor to GABA and GABACl blockers (Buckingham et al, 2005; Es-Salah et al., 2008; ffrench-Constant and Rocheleau, 1993; Hosie et al., 2001; Jones et al., 2009).

The macrocyclic lactone ivermectin B_{1a} is a positive allosteric modulator of GluCls (Ozoe, 2013). Ivermectin B_{1a} equally induced irreversible inward currents in a concentration-dependent fashion by acting on homomeric and heteromeric MdGluCls expressed in oocytes (Fig. 12). An X-ray crystallography study showed that Leu218, Ser260, and Thr285 of *C. elegans* GluCl-α at the subunit interface of the transmembrane domain are involved in binding ivermectin B_{1a} (Hibbs and Gouaux, 2011). These positions correspond to Ile249 [250], Ser292 [293], and Thr316 [317] of MdGluCls (Note that the numbers in brackets are for MdGluClC). A site-directed mutagenesis study indicated that amino acid residues of the GluCl (Hco-AVR-14B) of the nematode *Haemonchus contortus* involved in the binding of the macrocyclic lactone milbemycin A_4 are located at the interface between the extracellular and transmembrane domains

(Yamaguchi et al., 2012). These sites are distant from the exon 3-encoded region in the extracellular domain. These findings indicate that the difference of exon 3 does not affect the sensitivity to ivermectin B_{1a}, although the binding of ivermectin B_{1a} to GluCls is coupled to channel opening.

The GABACl blockers PTX and fipronil inhibit a glutamate-induced current by acting at GluCls (Eguchi et al., 2006; Ozoe et al., 2010; Zhao et al., 2004b). PTX and fipronil dose-dependently inhibited glutamate-induced currents in MdGluCls (Figs. 13A, 14A), with high nanomolar to high micromolar IC_{50}s. Homomeric MdGluClC channels are less sensitive to these blockers than homomeric MdGluClA and B channels (Figs. 13B and 14B). The low sensitivity of homomeric MdGluClC channels is not due to their excessive expression efficiency in oocytes because the same was observed even when the amount of injected cRNA was decreased (data not shown). The amino acid sequence of the putative binding site within the channel pore (Etter et al., 1999; Hibbs and Gouaux, 2011) is not responsible for the low sensitivity of MdGluClC channels because it is common between the variants. The tip of the β1/β2 loop, which contains a sequence corresponding to the exon 3-encoding region of MdGluCls, in the N-terminal extracellular domain forms a contact point with the extracellular end of the M2 segment and the M2-M3 linker of the channel domain (Miyazawa et al., 2003; Reeves et al., 2005). This interaction is crucial for the transduction of agonist binding to channel opening in Cys-loop receptors. The potencies of blockers could be influenced through this interaction. The MdGluClC subunit is longer than the other variants by one amino acid (Fig. 8A), and the amino acid sequence identities of the MdGluClC subunit with the MdGluClA and B subunits are 45.8% and 58.3%, respectively. It remains to be determined how these sequence differences between the MdGluClC subunit and the other variants affect the sensitivity to the channel blockers. All heteromeric channels, even channels containing MdGluClC, showed higher sensitivity to PTX compared with homomeric channels (Fig. 13). These findings suggest that MdGluCls in the central nervous system, which contains multiple MdGluCl subunit variants, might show high sensitivity to PTX, whereas peripheral MdGluCls predominantly comprised of variant C might show low sensitivity to PTX as well as fipronil. It was previously reported that PTX-sensitive and -insensitive GluCls co-exist in the dorsal unpaired median (DUM) neurons of the American cockroach (*Periplaneta americana*) (Raymond et al., 2000). Glutamate-induced currents recorded from the *P. americana* thoracic ganglion neurons are composed of two types of currents, desensitizing and non-desensitizing currents (Zhao et al., 2004a). Fipronil blocks both desensitizing and non-desensitizing currents, the latter (IC_{50} = 10 nM) being more sensitive to fipronil than the former (IC_{50} = 801

nM) (Zhao et al., 2004b). In this respect, it would be interesting to perform more detailed analysis of MdGluCls expressed in a cell line using patch clamp techniques.

In the present study, I have shown that *MdGluCl* are alternatively spliced to generate three variants (*A*-*C*). The transcripts of three variants are expressed in a spatially and temporally distinct manner. When expressed in *Xenopus* oocytes, functionally indistinguishable but pharmacologically distinct channels were formed. The physiological roles of differentially expressed variants remain to be examined.

Chapter 4

Effects of insecticides on glutamate- and GABA-gated chloride channels

Introduction

GABACls represent the important target of existing and emerging insecticides (phenylpyrazoles and benzamides) and ectoparasiticides such as A1443 (fluralaner) (Ozoe, 2013). GABACls are present in both vertebrates and invertebrates and mediate fast inhibitory neurotransmission. Insect ionotropic GABA receptors containing Rdl subunits are inhibited by fipronil, PTX, picrodendrin, bicyclophosphorothionates and ethynylbicycloorthobenzoate (EBOB) (Akiyoshi et al., 2013; Eguchi et al., 2006; ffrench-Constant and Rocheleau, 1993; Hosie et al., 1995, 1996; Nakao et al., 2013; Narusuye et al., 2007; Ozoe et al., 1998, 2010, 2013).

GluCls are present only in invertebrates such as insects and are the targets of insecticides and anthelmintics. GABA receptor antagonists, fipronil and PTX, inhibit glutamate-induced currents in GluCls (Eguchi et al., 2006; Kita et al., 2014; Ozoe et al., 2010; Zhao et al., 2004b). 3-Benzamido-*N*-phenylbenzamides (BPB) is a novel class of emerging insecticides that interacts with the GABACls with a different mode of action from that of conventional insecticides such as fipronil and PTX (Nakao et al., 2013; Ozoe et al., 2013). The macrocyclic lactone avermectins and ivermectins, which are positive allosteric modulators, induce irreversible currents and potentiate glutamate-induced currents in GluCls (Cully et al., 1994; Kita et al., 2014; McCavera et al., 2009). These compounds exhibit insecticidal and anthelmintic effects on insects and nematodes.

Both GABA and glutamate channels have been investigated by electrophysiological techniques such as patch-clamp and two-electrode voltage clamp (TEVC) to understand their pharmacological properties. Whereas many compounds block GABACls potently, compounds that specifically block GluCls are not known. In this chapter, I examined three selected bicyclophosphorothionates compounds and a BPB for their effects on MdGluCls and MdGABACls expressed in *Xenopus* oocytes using a TEVC technique.

Materials and methods

Chemicals

Sodium hydrogen L(+)-glutamate monohydrate, fipronil, and picrotoxinin (PTX) were purchased from Wako Pure Chemical Industries, Ltd. (Osaka, Japan). γ-Aminobutyric acid were purchased from Sigma-Aldrich (St. Louis, MO). Bicyclophosphorothionates, *tert*-butylbicyclophosphorothionate (TBPS), 4-isobutyl-3-isopropylbicyclophosphorothionate (PS-14) and 1-hydroxyethylphosphorothionate (1HEPS) were synthesized in this laboratory. BPB 1 (Meta-diamide 1) was donated by Mitsui chemicals Agro Inc. (Chiba, Japan).

Animals

Mature female African clawed frogs (*Xenopus laevis*) used all experiments were purchased from Shimizu Laboratory Supplies Co., Ltd. (Kyoto, Japan).

cRNA preparation and injection into Xenopus oocytes

Three *MdGluCl* variants (Kita et al, 2014) and *MdRdl* were amplified by PCR using KOD -Plus- NEO (Toyobo Co., Ltd.), pcDNA3-*MdGluClA* (DDBJ accession no. AB177546), -*MdGluClB* (AB698079), -*MdGluClC* (AB698080) or –$MdRdl_{ac}$ (DDBJ accession nos. AB824728 and AB824729) as templates, and the primers pcDNA3-cRNAF (5'-CTCTCTGGCTAACTAGAGAACC-3') and pcDNA3-cRNAR (5'-AACTAGAAGGCACAGTCGAG-3'). The PCR products were purified using the illustra™ GFX™ PCR DNA and Gel Band Purification Kit (GE Healthcare UK, Ltd., Little Chalfont, UK), and their DNA sequences were confirmed. The capped RNAs were synthesized by T7 polymerase, using the mMESSAGE mMACHINE® T7 Ultra Kit (Ambion, Austin, TX) and 100 ng of purified PCR products. The quality and quantity of synthesized cRNAs were assessed by agarose gel electrophoresis and absorption spectroscopy. The synthesized cRNAs were stored at -20 °C until use.

Mature female *X. laevis* was anesthetized with 0.1% (w/v) ethyl *m*-aminobenzoate methanesulfonate (Wako Pure Chemical Industries, Ltd.), and the ovarian lobes were dissected out. The ovarian lobes were treated with collagenase (2 mg/ml; Sigma-Aldrich) in Ca^{2+}-free standard oocyte solution (SOS) (100 mM NaCl, 2 mM KCl, 1 mM $MgCl_2$, 5 mM HEPES, pH 7.6) for 60-120 min at room temperature. After the

treatment, the oocytes were gently washed with SOS (100 mM NaCl, 2 mM KCl, 1 mM $MgCl_2$, 1.8 mM $CaCl_2$, 5 mM HEPES, pH 7.6) containing 2.5 mM sodium pyruvate, gentamycin (50 μg/ml; Gibco, Langley, OK), penicillin (100 U/ml; Invitrogen) and streptomycin (100 μg/ml; Invitrogen), and they were incubated in the same buffer at 16 °C overnight. The oocytes were injected with 30 ng of each cRNA for analysis of channel functions and incubated under the same conditions for one day.

Two-electrode voltage-clamp recordings

The glutamate-induced currents were recorded by a TEVC method using an Oocyte Clamp OC-725C amplifier (Warner Instruments, Hamden, CT). The oocytes were kept in SOS and clamped at a membrane potential of -80 mV. The glass capillary electrodes were filled with 2 M KCl and had a resistance of 0.5-1.5 MΩ. The recorded currents were analyzed using Data-Trax2^{TM} software (World Precision Instruments Inc., Sarasota, FL). The experiments were performed at 18-22 °C. Glutamate and GABA were dissolved in SOS and applied to the oocytes for 3 s. After the glutamate or GABA application, the oocytes were washed by SOS for more than 30 s and assessed for their integrity. TBPS, PS-14, 1HEPS and BPB 1 were first dissolved in DMSO and then diluted 10 μM with SOS. Glutamate or GABA at 10 μM was first applied to oocytes several times to get a control response. The blocker solution containing 0.1% DMSO was perfused for 3-10 min until a stable inhibition of the glutamate response was reached. The inhibition percentage was calculated from the average of two minimum responses to 10 μM glutamate or 10 μM GABA during the perfusion of a blocker. Fifty percent effective concentrations (EC_{50}s), Hill coefficients (n_Hs), and fifty percent inhibitory concentrations (IC_{50}s) were obtained from concentration-response relationships by nonlinear regression analysis using OriginPro 8J (Origin Lab, Northampton, MA). These values are presented as mean ± SEM.

Statistics

Data are presented as mean ± SEM determined from at least three separate experiments. Significance was analyzed using unpaired Student's *t*-test.

Results

Effects of bicyclophosphorothionates on MdGluCls

Three bicyclophosphorothionate GABA receptor antagonists, TBPS, PS-14, and 1HEPS (Fig. 15), which bind to the non-competitive binding site in the M2 domain of GABACls. These compounds were examined for their antagonistic effects on MdGluCls expressed in *Xenopus* oocytes using a TEVC tequnique (Fig. 16). TBPS, PS-14, and 1HEPS hardly inhibited glutamate-induced currents or were without effects. TBPS at 10 μM produced 4.83 ± 2.75%, -1.76 ± 4.75% and 5.61 ± 2.44% inhibition of the response to 10 μM glutamate in MdGluClA, B and C, respectively. PS-14 produced 0.74 ± 5.50%, 4.81 ± 2.05% and 3.78 ± 4.28% inhibition in MdGluClA, B and C, respectively. 1HEPS produced 9.53 ±2.88%, 7.82 ± 1.17 and -3.49 ± 2.76% in MdGluClA, B and C, respectively.

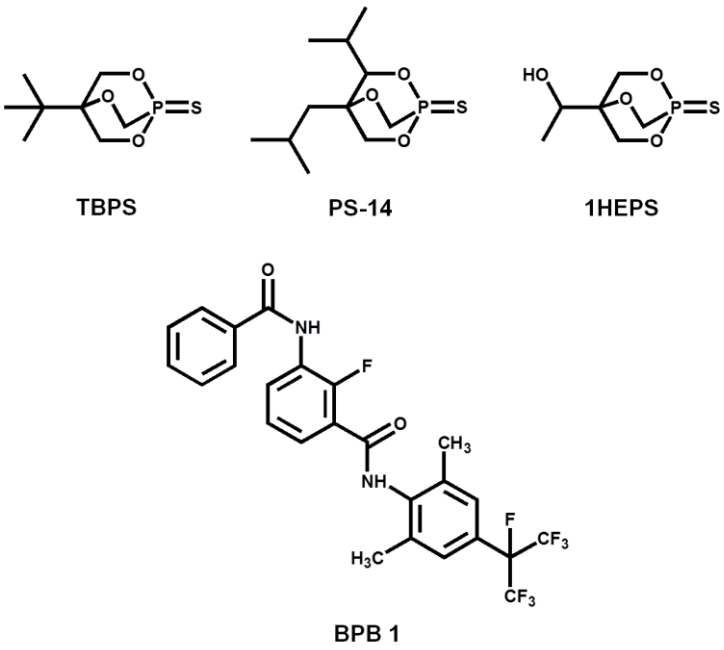

Fig. 15. Structures of bicyclophosphorothionates and BPB 1.

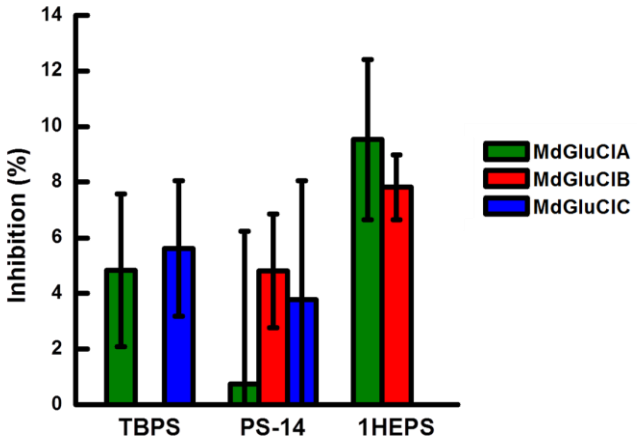

Fig. 16. Inhibition of glutamate-induced currents by bicyclophosphorothionates in three MdGluCl variants.

All compounds were tested at 10 μM. Data are means ± SEM (n=3).

Effects of BPB 1 on MdGABACl and MdGluCl

Inhibitory effects of BPB 1 on GABACls ($MdRdl_{ac}$) and GluCls (MdGluClA) expressed in *Xenopus* oocytes were examined using a TEVC technique (Fig. 17). BPB 1 at 100 nM potently inhibited GABA-gated currents in oocytes injected with $MdRdl_{ac}$ cRNA (Fig. 17A), whereas BPB 1 at 10 μM showed little inhibition of MdGluClA channels (Fig. 17B). The dose-response curves of BPB 1 for MdGABACls containing $MdRdl_{ac}$ gave an IC_{50} of 12.0 ± 1.2 nM (Fig. 17C).

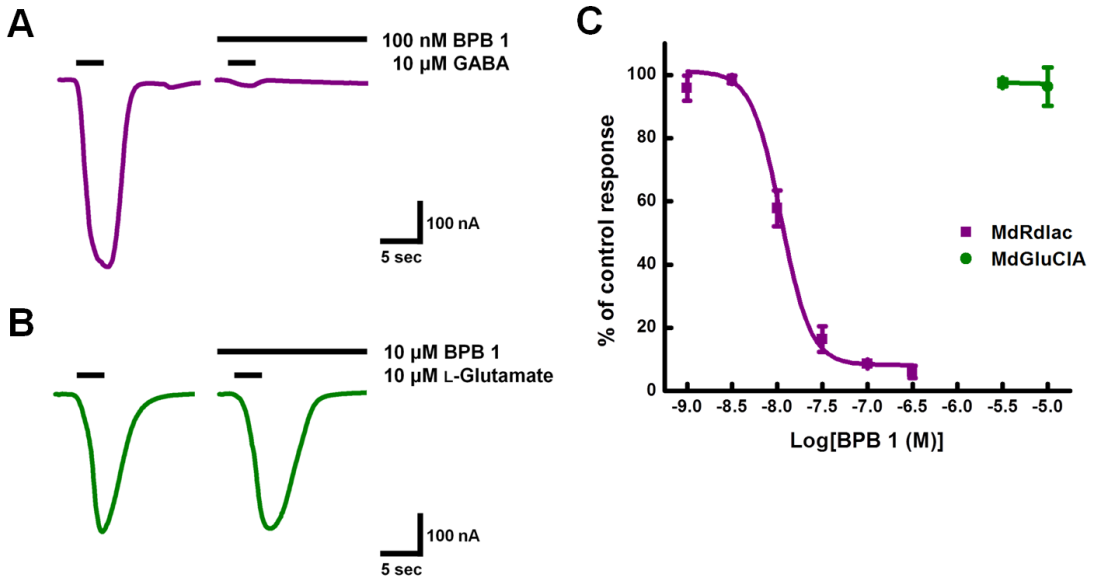

Fig. 17. Effects of BPB 1 on housefly GABACl and GluCl expressed in *Xenopus* oocytes.

(A) GABA-induced currents in $MdRdl_{ac}$. (B) L-Glutamate-induced currents in MdGluClA. (C) Dose -response curve of the inhibition of GABA-induced currents by BPB 1. Data are expressed as mean ± SE from at least six oocytes from two frogs.

Discussion

The GABA receptor antagonists, fipronil and PTX, inhibit glutamate-induced currents on GluCls (Eguchi et al., 2006; Kita et al., 2014; Zhao et al., 2004b). Fipronil and PTX blocked MdGluCls, and the dose-response curves gave IC_{50}s of 746 ± 214 nM and 67.1 ± 8.6 μM in MdGluClA, respectively (Chapter 2). In MdGABACl containig $MdRdl_{bd}$ subunits, the dose-response curves of fipronil and PTX gave IC_{50}s of 3.02 and 46.8 nM (Eguchi et al., 2006). These GABA receptor antagonists potently inhibited MdGABACls compared to MdGluCls.

GABACls are the target of bicyclophosphorothionates such as TBPS, PS-14, and 1HEPS (Akiyoshi et al., 2013; Eto et al., 1976). TBPS acts at mammalian $GABA_A$ receptors most potentlys, whereas PS-14 selectively acts at insect GABA receptors because of bearing an isopropyl group at the 3-position (Ju et al., 2010). 1HEPS has a hydrophilic substituent at the bridge head, whereas TBPS has a hydrophobic substituent. This compound was chosen as the hydrophilic (a 1-hydroxyethyl) substituent of 1HEPS was assumed to interact with the hydrophilic amino acid at the 2' position of the M2 of MdGluCls (the putative binding site). I examined whether these three different types of

compounds inhibit MdGluCls. Three bicyclophosphorothionates showed weak or no inhibition (less than 10%) in three MdGluCls containing MdGluClA, B, and C (Fig. 16). These results suggested that GluCls are not the target of bicyclophosphorothionates, although bicyclophosphorothionates selectively block GABACls.

3-Benzamido-*N*-phenylbenzamides (BPBs) have recently been identified as insecticides. BPBs likely act at a distinct site in insect GABACls (Nakao et al., 2013). I examined whether BPB 1 blocks MdGABACls and MdGluClA channels. BPB 1 potently inhibited GABA-induced currents in GABACls, whereas BPB 1 hardly inhibited glutamate-induced currents in MdGluClA channels. The binding site of BPB 1 was proposed to be located in the subunit interface between transmembrane domains M1 and M3 (Nakao et al., 2013). It was reported that Gly336 of the *Drosophila* Rdl subunit is important for binding BPBs. Gly336 corresponds to Gly333 of $MdRdl_{ac}$ and Gly312 of MdGluClA; equivalent Gly is conserved in both subunits. However, the sensitivity of BPB 1 was different between MdGABACls and MdGluClA channels.
The pharmacological properties of GluCls were compared with those of GABACls using several antagonists in this study. GABACls are the established target of many GABA receptor blockers. The data indicate thatGluCls are not target of GABA receptor blockers such as bicyclophosphorothionates and BPB 1. As many GABA receptor antagonists have been identified to date, these compounds also need to be investigated for their antagonism of GluCls to examine whether GluCls are a target for novel insect control chemicals.

Chapter 5

Final conclusions

Both GluCls and GABACls mediate inhibitory neurotransmission in invertebrates such as insects and are the targets of insecticides. I first investigated the expression levels of two genes that encode MdGluCl and MdRdl by real-time qPCR and [^{3}H]ligand binding assay to understand channel localization. The highest expression of *MdGluCl* and *MdRdl* were detected in the adult housefly head containing central nervous tissues. *MdGluCl* is alternatively spliced into three variants. Two variants termed *MdGluClA* and *MdGluClB* were highly expressed in the adult head. Interestingly, the expression level of *MdGluCl* in the adult legs was higher than *MdRdl*. *MdGluClC,* which is an exon 3 splice variant was exclusively expressed in the adult leg and abdomen. The GluCls expressed in the legs and abdomen are likely the variant-C homopentamer because the MdGluClC transcript was exclusively enriched in these tissues.

Immunohistochemical analysis showed that MdGluCl subunits were mainly distributed in the lamina, medulla, the retina basement membrane, and the pigment cells beneath the lens in the optic lobe. MdGluCls were located in the motor neuron cell bodies clustered anterior and posterior to the thoracic neuropils, while MdRdl subunits were located in the neuropile of the thoracic ganglion. MdGluCl immunoreactivity was detected in the legs. MdRdl channels were widely distributed in the optic lobe such as medulla, lobula, lobula plate of the adult brain. Tissue localizations of these channels in the brain, thorax and legs were different. These results suggest that these similar ionotropic receptors contribute to inhibitory neurotransmission in different physiological processes in the housefly.

Three types of *MdGluCl* variants, which are generated by alternative splicing, showed similar electrophysiological properties in terms of glutamate sensitivity (EC_{50}) and Hill coefficient (n_H) when expressed in *Xenopus* oocytes. There were no difference between homopentameric channels of these variants and co-expressed channels. The positive allosteric GluCl modulator ivermectin B_{1a} induced dose-dependent, irreversible currents in channels, when the subunit variants are singly expressed and co-expressed in oocytes. However, there were no significant difference in ivermectin sensitivity and induced currents. Pharmacological properties of MdGluCl variants were examined using the GABA receptor antagonists PTX and fipronil. MdGluClA and B channels

showed similar properties, whereas MdGluClC channels were less sensitive to these compounds than A and B channels. The channels expressed by injecting more than two splice variant cRNAs revealed almost the same sensitivities to these antagonists. These results suggest that exon 3 of MdGluCl does not affect glutamate and ivermectin sensitivity, and channel functions, but alter antagonist sensitivities. MdGluCls in the central nervous system, which expresses different MdGluCl subunit variants, might show high sensitivity to PTX, whereas peripheral MdGluCls predominantly comprised of variant C might show low sensitivity to PTX as well as fipronil.

The GABA receptor blockers bicyclophosphorothionates (TBPS, PS-14, and 1HEPS) and BPB 1 showed little inhibition of MdGluCls. These results suggest that GluCls are not the target of these GABA receptor blockers.

In conclusion, GluCls and GABACls are important for inhibitory neurotransmission in invertebrates, and are the target of insecticides. Localizations of GluCls and GABACls were different. This finding suggests that GluCls play different roles from GABACls. Three MdGluCl splice variants differed in their expression levels and expression sites. These results suggest that MdGluCls regulate inhibitory neurotransmission in different body part and tissues by expressing splice variants. Further studies are needed to clarify the mechanisms underlying the different antagonist sensitivities of GluCl variants, and to identify compounds which selectively act on GluCls as both agonists and antagonists, which would be useful for research tools and practical insecticides.

Acknowledgements

The work presented here is the result of a great many of people's support. I would like to thank Professor Yoshihisa Ozoe, Department of Life Science and Biotechnology, Faculty of Life and Environmental Science, Shimane University, for kind advices and warm encouragement. Without his support, I would not be completing this work. It has been my very good fortune to work in my laboratory filled with so many good people. Without Mrs. Ozoe I would not have known where to begin my research. She patiently taught me nearly all of the techniques used in this study about molecular biology and biochemistry. Professor Masaaki Azuma, Division of Bioscience and Biotechnology, the United Graduate school of Agricultural Science, Tottori University, gave me useful advices about techniques of immunohistochemistry, and discussed with me about the latest progress in this study. I would like to thank Dr. Kohji Nishimura, Department of Molecular and Functional Genomics, Center for Integrated Research in Science, Shimane University, for his kind advices and guidance in this work. Finally, I would like to thank Dr. Izumi Ikeda and Kenjiro Furuta, and all other lab members for warm encouragement.

References

Akiyoshi, Y., Ju, X.-L., Furutani, S., Matsuda, K., Ozoe, Y., 2013. Electrophysiological evidence for 4-isobutyl-3-isopropylbicyclophosphorothionate as a selective blocker of insect GABA-gated chloride channels. Bioorg. Med. Chem. Lett. 23, 3373-3376.

Aronstein, K., ffrench-Constant, R.H., 1995. Immunocytochemistry of a novel GABA receptor subunit *Rdl* in *Drosophila melanogaster*. Invert. Neurosci. 1, 25-31.

Awapara, J., Landua, A.J., Fuerst, R., Seale, B, 1950. Free γ-aminobutyric acid in brain. J. Biol. Chem. 187, 35-39.

Baek, M., Mann, R.S., 2009. Lineage and birth date specify motor neuron targeting and dendritic architecture in adult *Drosophila*. J. Neurosci. 29, 6904-6916.

Barbara, G.S., Zube, C., Rybak, J., Gauthier, M., Grünewald, B., 2005. Acetylcholine, GABA and glutamate induce ionic currents in cultured antennal lobe neurons of the honeybee, *Apis mellifera*. J. Comp. Physiol. A 191, 823-836.

Bloomquist, J.G., 1994. Cyclodiene resistance at the insect GABA receptor/chloride channel complex confers broad cross resistance to convulsants and experimental phenylpyrazole insecticides. Arch. Insect Biochem. Physiol. 26, 69-79.

Boerner, J., Duch, C., 2010. Average shape standard for the adult *Drosophila* ventral nerve cord. J. Comp. Neurol. 518, 2437-2455.

Boumghar, K., Couret-Fauvel, T., Garcia, M., Armengaud, C., 2012. Evidence for a role of GABA- and glutamate-gated chloride channels in olfactory memory. Pharmacol. Biochem. Behav. 103, 69-75.

Bradford, M.M., 1976. A rapid and sensitive method for the quantitation of microgram quantities of protein utilizing the principle of protein-dye binding. Anal. Biochem. 72, 248-254.

Brierley, D.J., Rathore, K., VijayRaghavan, K., Williams, D.W., 2012. Developmental origins and architecture of *Drosophila* leg motoneurons. J. Comp. Neurol. 520, 1629-1649.

Buckingham, S.D., Biggin, P.C., Sattelle, B.M., Brown, L.A., Sattelle, D.B., 2005. Insect GABA receptors: splicing, editing, and targeting by antiparasitics and insecticides. Mol. Pharmacol. 68, 942-951.

Cayre, M., Buckingham, S.D., Yagodin, S., Sattelle, D.B., 1999. Cultured insect mushroom body neurons express functional receptors for acetylcholine, GABA, glutamate, octopamine, and dopamine. J. Neurophysiol. 81, 1-14.

Collins, B., Kane, E.A., Reeves, D.C., Akabas, M.H., Blau, J., 2012. Balance of activity

between LNvs and glutamatergic dorsal clock neurons promotes robust circadian rhythms in *Drosophila*. Neuron 74, 706-718.

Cull-Candy, S.G., 1976. Two types of extrajunctional L-glutamate receptors in locust muscle fibres. J. Physiol. 255, 449-464.

Cull-Candy, S.G., Usherwood, P.N.R., 1973. Two populations of L-glutamate receptors on locust muscle fibres. Nature 246, 62-64.

Cully, D.F., Vassilatis, D.K., Liu, K.K., Paress, P.S., Van der Ploeg, L.H., Schaeffer, J.M., Arena, J.P., 1994. Cloning of an avermectin-sensitive glutamate-gated chloride channel from *Caenorhabditis elegans*. Nature 371, 707-711.

Cully, D.F., Paress, P.S., Liu, K.K., Schaeffer, J.M., Arena, J.P., 1996. Identification of a *Drosophila melanogaster* glutamate-gated chloride channel sensitive to the antiparasitic agent avermectin. J. Biol. Chem. 271, 20187-20191.

Delgado, R., Barla, R., Latorre, R., Labarca, P., 1989. L-Glutamate activates excitatory and inhibitory channels in *Drosophila* larval muscle. FEBS Letters 243, 337-342.

Démares, F., Raymond, V., Armengaud, C., 2013. Expression and localization of glutamate-gated chloride channel variants in honeybee brain (*Apis mellifera*). Insect Biochem. Mol. Biol. 43, 115-124.

Eguchi, Y., Ihara, M., Ochi, E., Shibata, Y., Matsuda, K., Fushiki, S., Sugama, H., Hamasaki, Y., Niwa, H., Wada, M., Ozoe, F., Ozoe, Y., 2006. Functional characterization of *Musca* glutamate- and GABA-gated chloride channels expressed independently and coexpressed in *Xenopus* oocytes. Insect Mol. Biol. 15, 773-783.

El Hassani, A.K., Schuster, S., Dyck, Y., Demares, F., Leboulle, G., Armengaud, C., 2012. Identification, localization and function of glutamate-gated chloride channel receptors in the honeybee brain. Eur. J. Neurosci. 36, 2409-2420.

Enell, L., Hamasaka, Y., Kolodziejczyk, A., Nässel, D.R., 2007. γ-Aminobutyric acid (GABA) signaling components in *Drosophila*: immunocytochemical localization of $GABA_B$ receptors in relation to the $GABA_A$ receptor subunit RDL and a vesicular GABA transporter. J. Comp. Neurol. 505, 18-31.

Es-Salah, Z., Lapied, B., Le Goff, G., Hamon, A., 2008. RNA editing regulates insect gamma-aminobutyric acid receptor function and insecticide sensitivity. NeuroReport 19, 939-943.

Eto, M., Ozoe, Y., Fujita, T., Casida, J.E., 1976. Significance of branched bridge-head substituent in toxicity of bicyclic phosphate esters. Agric. Biol. Chem. 40, 2113-2115.

Etter, A., Cully, D.F., Liu, K.K., Reiss, B., Vassilatis, D.K., Schaeffer, J.M., Arena, J.P., 1999. Picrotoxin blockade of invertebrate glutamate-gated chloride channels:

subunit dependence and evidence for binding within the pore. J. Neurochem. 72, 318-326.

ffrench-Constant, R.H., Mortlock, D.P., Shaffer, C.D., Macintyre, R.J., Roush, R.T., 1991. Molecular cloning and transformation of cyclodiene resistance in *Drosophila*: an invertebrate γ-aminobutyric acid subtype A receptor locus. Proc. Natl. Acad. Sci. USA 88, 7209-7213.

ffrench-Constant, R.H., Rocheleau, T.A., 1993. *Drosophila* γ-aminobutyric acid receptor gene *Rdl* shows extensive alternative splicing. J. Neurochem. 60, 2323-2326.

ffrench-Constant, R.H., Rocheleau, T.A., Steichen, J.C., Chalmers, A.E., 1993. A point mutation in a *Drosophila* GABA receptor confers insecticide resistance. Nature 363, 449-451.

Fraser, S.P., Djamgoz, M.B.A., Usherwood, P.N.R., O'Brien, J., Darlison, M.G., Barnard, E.A., 1990. Amino acid receptors from insect muscle: electrophysiological characterization in *Xenopus* oocytes following expression by injection of mRNA. Mol. Brain Res. 8, 331-341.

Gisselmann, G., Pusch, H., Hovemann, B.T., Hatt, H., 2002. Two cDNAs coding for histamine-gated ion channels in *D. melanogaster*. Nat. Neurosci. 5, 11-12.

Gisselmann, G., Plonka, J., Pusch, H., Hatt, H., 2004. *Drosophila melanogaster* GRD and LCCH3 subunits form heteromultimeric GABA-gated cation channels. Br. J. Pharmacol. 142, 409-413.

Hall, Z.W., 1992. An Introduction to Molecular Neurobiology. Sinauer Associates, Sunderland, MA, pp. 555.

Harrison, J.B., Chen, H.H., Sattelle, E., Barker, P.J., Huskisson, N.S., Rauh, J.J., Bai, D., Sattelle, D.B., 1996. Immunocytochemical mapping of a C-terminus anti-peptide antibody to the GABA receptor subunit, RDL in the nervous system of *Drosophila melanogaster*. Cell Tissue Res. 284, 269-278.

Harvey, R.J., Schmitt, B., Hermans-Borgmeyer, I., Gundelfinger, E.D., Betz, H., Darlison, M.G., 1994. Sequence of a *Drosophila* ligand-gated ion-channel polypeptide with an unusual amino-terminal extracellular domain. J. Neurochem. 62, 2480-2483.

Henderson, J.E., Soderlund, D.M., Knipple, D.C., 1993. Characterization of a putative gamma-aminobutyric acid (GABA) receptor β subunit gene from *Drosophila melanogaster*. Biochem. Biophys. Res. Commun. 193, 474-482.

Hibbs, R.E., Gouaux, E., 2011. Principles of activation and permeation in an anion-selective Cys-loop receptor. Nature 474, 54-60.

Højland, D.H., Scott, J.G., Jensen, K.M., Kristensen, M., 2013. Autosomal male

determination in a spinosad-resistant housefly strain from Denmark. Pest Manag. Sci., doi: 10.1002/ps.3655.

Hosie, A.M., Baylis, H.A., Buckingham, S.D., Sattelle, D.B., 1995. Actions of the insecticide fipronil, on dieldrin-sensitive and- resistant GABA receptors of *Drosophila melanogaster*. Br. J. Pharmacol. 115, 909-912.

Hosie, A.M., Ozoe, Y., Koike, K., Ohmoto, T., Nikaido, T., Sattelle, D.B., 1996. Actions of picrodendrin antagonists on dieldrin-sensitive and -resistant *Drosophila* GABA receptors. Br. J. Pharmacol. 119, 1569-1576.

Hosie, A.M., Buckingham, S.D., Presnail, J.K., Sattelle, D.B., 2001. Alternative splicing of a *Drosophila* GABA receptor subunit gene identifies determinants of agonist potency. Neuroscience 102, 709-714.

Ihara, M., Ishida, C., Okuda, H., Ozoe, Y., Matsuda, K., 2005. Differential blocking actions of 4'-ethynyl-4-*n*-propylbicycloorthobenzoate (EBOB) and γ-hexachlorocyclohexane (γ-HCH) on γ-aminobutyric acid- and glutamate-induced responses of American cockroach neurons. Invert. Neurosci. 5, 157-164.

Janssen, D., Derst, C., Buckinx, R., Van den Eynden, J., Rigo, J.-M., Van Kerkhove, E., 2007. Dorsal unpaired median neurons of *Locusta migratoria* express ivermectin- and fipronil-sensitive glutamate-gated chloride channels. J. Neurophysiol. 97, 2642-2650.

Janssen, D., Derst, C., Rigo, J.-M., Van Kerkhove, E., 2010. Cys-loop ligand-gated chloride channels in dorsal unpaired median neurons of *Locusta migratoria*. J. Neurophysiol. 203, 2587-2598.

Jensen, M.L., Schousboe, A., Ahring, P.K., 2005. Charge selectivity of the Cys-loop family of ligand-gated ion channels. J. Neurochem. 92, 217-225.

Jepson, J.E.C., Reenan, R.A., 2007. Genetic approaches to studying adenosine-to-inosine RNA editing. Methods Enzymol. 424, 265-287.

Jones, A.K., Sattelle, D.B., 2007. The cys-loop ligand-gated ion channel gene superfamily of the red flour beetle, *Tribolium castaneum*. BMC Genomics 8, 327.

Jones, A.K., Sattelle, D.B., 2008. The cys-loop ligand-gated ion channel gene superfamily of the nematode, *Caenorhabditis elegans*. Invert. Neurosci. 8, 41-47.

Jones, A.K., Buckingham, S.D., Papadaki, M., Yokota, M., Sattelle, B.M., Matsuda, K., Sattelle, D.B., 2009. Splice-variant- and stage-specific RNA editing of the *Drosophila* GABA receptor modulates agonist potency. J. Neurosci. 29, 4287-4292.

Ju, X.-L., Fusazaki, S., Hishinuma, H., Qiao, X., Ikeda, I., Ozoe, Y., 2010. Synthesis and structure-activity relationship analysis of bicyclophosphorothionate blockers with selectivity for housefly γ-aminobutyric acid receptor channels. Pest Manag.

Sci. 66, 1002-1010.

Kane, N.S., Hirschberg, B., Qian, S., Hunt, D., Thomas, B., Brochu, R., Ludmerer, S.W., Zheng, Y., Smith, M., Arena, J.P., Cohen, C.J., Schmatz, D., Warmke, J., Cully, D.F., 2000. Drug-resistant *Drosophila* indicate glutamate-gated chloride channels are targets for the antiparasitics nodulisporic acid and ivermectin. Proc. Natl. Acad. Sci. USA 97, 13949 -13954.

Keegan, L.P., Gallo, A., O'Connell, M.A., 2001. The many roles of an RNA editor. Nat. Rev. Genet. 2, 869-878.

Khan, H.A., Akram, W., Shad, S.A. Lee, J.J., 2013. Insecticide mixtures could enhance the toxicity of insecticides in a resistant dairy population of *Musca domestica* L. PLoS One 8, e60929.

Kita, T., Ozoe, F., Azuma, M., Ozoe, Y., 2013. Differential distribution of glutamate- and GABA-gated chloride channels in the housefly *Musca domestica*. J. Insect Physiol. 59, 887-893.

Kita, T., Ozoe, F., Ozoe, Y., 2014. Expression pattern and function of alternative splice variants of glutamate-gated chloride channel in the housefly *Musca domestica*. Insect Biochem. Mol. Biol. 45, 1-10.

Kolodziejczyk, A., Sun, X., Meinertzhagen, I.A., Nässel, D.R., 2008. Glutamate, GABA and acetylcholine signaling components in the lamina of the *Drosophila* visual system. PLoS One 3, e2110.

Kornblihtt, A.R., Schor, I.E., Alló, M., Dujardin, G., Petrillo, E., Muñoz, M.J., 2013. Alternative splicing: a pivotal step between eukaryotic transcription and translation. Nat. Rev. Mol. Cell Biol. 14, 153-165.

Kral, K., Meinertzhagen, I.A., 1989. Anatomical plasticity of synapses in the lamina of the optic lobe of the fly. Philos. Trans. R. Soc. B 323, 155-183.

Kwon, D.H., Yoon, K.S., Clark, J.M., Lee, S.H., 2010. A point mutation in a glutamate-gated chloride channel confers abamectin resistance in the two-spotted spider mite, *Tetranychus urticae* Koch. Insect Mol. Biol. 19, 583-591.

Lee, D., Su, H., O'Dowd, D.K., 2003. GABA receptors containing Rdl subunits mediate fast inhibitory synaptic transmission in *Drosophila* neurons. J. Neurosci. 23, 4625-4634.

Li, Q., Lee, J.-A., Black, D.L., 2007. Neuronal regulation of alternative pre-mRNA splicing. Nat. Rev. Neurosci. 8, 819-831.

Liu, H.-P., Lin, S.-C., Lin, C.-Y., Yeh, S.-R., Chiang, A.-S., 2005. Glutamate-gated chloride channels inhibit juvenile hormone biosynthesis in the cockroach, *Diploptera punctata*. Insect Biochem. Mol. Biol. 35, 1260-1268.

Liu, W.W., Wilson, R.I., 2013. Glutamate is an inhibitory neurotransmitter in the *Drosophila* olfactory system. Proc. Natl. Acad. Sci. UAS 110, 10294-10299.

Marshall, J., Buckingham, S.D., Shingai, R., Lunt, G.G., Goosey, M.W., Darlison, M.G., Sattelle, D.B., Barnard, E.A., 1990. Sequence and functional expression of a single α subunit of an insect nicotinic acetylcholine receptor. EMBO J. 9, 4391-4398.

McCarthy, E.v., Wu, Y., deCarvalho, T., Brandt, C., Cao, G., Nitabach, M.N., 2011. Synchronized bilateral synaptic inputs to *Drosophila melanogaster* neuropeptidergic rest/arousal neurons. J. Neurosci. 31, 8181-8193.

McCavera, S., Rogers, A.T., Yates, D.M., Woods, D.J., Wolstenholme, A.J., An ivermectin-sensitive glutamate-gated chloride channel from the parasitic nematode *Haemonchus contortus*. Mol. Pharmacol. 75, 1345-1355.

Meinertzhagen, I.A., O'Neil, S.D., 1991. Synaptic organization of columnar elements in the lamina of the wild type in *Drosophila melanogaster*. J. Comp. Neurol. 305, 232-263.

Miyazawa, A., Fujiyoshi, Y., Unwin, N., 2003. Structure and gating mechanism of the acetylcholine receptor pore. Nature 423, 949-955.

Nakao, T., Banba, S., Nomura, M., Hirase, K., 2013. Meta-diamide insecticides acting on distinct sites of RDL GABA receptor from those for conventional noncompetitive antagonists. Insect Biochem. Mol. Biol. 43, 366-375.

Narahashi, T., Zhao, X., Ikeda, T., Salgado, V.L., Yeh, J.Z., 2010. Glutamate-activated chloride channels: unique fipronil targets present in insects but not in mammals. Pestic. Biochem. Physiol. 97, 149-152.

Narusuye, K., Nakao, T., Abe, R., Nagatomi, Y., Hirase, K., Ozoe, Y., 2007. Molecular cloning of a GABA receptor subunit from *Laodelphax striatella* (Fallén) and patch clamp analysis of the homo-oligomeric receptors expressed in a *Drosophila* cell line. Insect Mol. Biol. 16, 723-733.

Okada, R., Awasaki, T., Ito, K., 2009. Gamma-aminobutyric acid (GABA)-mediated neural connections in the *Drosophila* antennal lobe. J. Comp. Neurol. 514, 74-91.

Ozoe, Y., 2013. γ-Aminobutyrate- and glutamate-gated chloride channels as targets of insecticides. Adv. Insect Physiol. 44, 211-286.

Ozoe, Y., Akamatsu, M., Higata, T., Ikeda, I., Mochida, K., Koike, K., Ohmoto, T., Nikaido, T., 1998. Picrodendrin and related terpenoid antagonists reveal structural differences between ionotropic GABA receptors of mammals and insects. Bioorg. Med. Chem. 6, 481-492.

Ozoe, Y., Asahi, M., Ozoe, F., Nakahira, K., Mita, T., 2010. The antiparasitic isoxazoline A1443 is a potent blocker of insect ligand-gated chloride channels.

Biochem. Biophys. Res. Commun. 391, 744-749.

Ozoe, Y., Kita, T., Ozoe, F., Nakao, T., Sato, K., Hirase, K., 2013. Insecticidal 3-benzamido-*N*-phenylbenzamides specifically bind with high affinity to a novel allosteric site in housefly GABA receptors. Pestic. Biochem. Physiol. 107, 285-292.

Pirri, J.K., McPherson, A.D., Donnelly, J.L., Francis, M.M., Alkema, M.J., 2009. A tyramine-gated chloride channel coordinates distinct motor programs of a *Caenorhabditis elegans* escape response. Neuron 62, 526-538.

Putrenko, I., Zakikhani, M., Dent, J.A., 2005. A family of acetylcholine-gated chloride channel subunits in *Caenorhabditis elegans*. J. Biol. Chem. 280, 6392-6398.

Raghu, S.V., Borst, A., 2011. Candidate glutamatergic neurons in the visual system of *Drosophila*. PLoS One 6, e19472.

Ranganathan, R., Cannon, S.C., Horvitz, H.R., 2000. MOD-1 is a serotonin-gated chloride channel that modulates locomotory behaviour in *C. elegans*. Nature 408, 470-475.

Raymond, V., Sattelle, D.B., Lapied, B., 2000. Co-existence in DUM neurones of two GluCl channels that differ in their picrotoxin sensitivity. NeuroReport 11, 2695-2701.

Reeves, D.C., Jansen, M., Bali, M., Lemster, T., Akabas, M.H., 2005. A role for the β_1-β_2 loop in the gating of 5-HT_3 receptors. J. Neurosci. 25, 9358-9366.

Scott, J.G., Liu, N., Kristensen, M., Clark, A.G., 2009. A case for sequencing the genome of *Musca domestica* (Diptera: Muscidae). J. Med. Entomol. 46, 175-182.

Semenov, E.P., Pak, W.L., 1999. Diversification of *Drosophila* chloride channel gene by multiple posttranscriptional mRNA modifications. J. Neurochem. 72, 66-72.

Sinakevitch, I., Strausfeld, N.J., 2004. Chemical neuroanatomy of the fly's movement detection pathway. J. Comp. Neurol. 468, 6-23.

Soler, C., Daczewska, M., Da Ponte, J.P., Dastugue, B., Jagla, K., 2004. Coordinated development of muscles and tendons of the *Drosophila* leg. Development 131, 6041-6051.

Takemura, S., Karuppudurai, T., Ting, C.-Y., Lu, Z., Lee, C.-H., Meinertzhagen, I.A., 2011. Cholinergic circuits integrate neighboring visual signals in a *Drosophila* motion detection pathway. Curr. Biol. 21, 2077-2084.

Usherwood, P.N.R., Grundfest, H., 1964. Inhibitory postsynaptic potentials in grasshopper muscle. Science 143, 817-818.

Usherwood, P.N.R., Grundfest, H., 1965. Peripheral inhibition in skeletal muscle of insects. J. Neurophysiol. 28, 497-518.

Yamaguchi, M., Sawa, Y., Matsuda, K., Ozoe, F., Ozoe, Y., 2012. Amino acid residues

of both the extracellular and transmembrane domains influence binding of the antiparasitic agent milbemycin to *Haemonchus contortus* AVR-14B glutamate-gated chloride channels. Biochem. Biophys. Res. Commun. 419, 562-566.

Wafford, K.A., Sattelle, D.B., 1989. L-Glutamate receptors on the cell body membrane of an identified insect motor neurone. J. Exp. Biol. 144, 449-462.

Zhang., H.-G., ffrench-Constant, R.H., Jackson, M.B., 1994. A unique amino acid of the *Drosophila* GABA receptor with influence on drug sensitivity by two mechanisms. J. Physiol. 479, 65-75.

Zhao, X., Salgado, V.L., Yeh, J.Z., Narahashi, T., 2004a. Kinetic and pharmacological characterization of desensitizing and non-desensitizing glutamate-gated chloride channels in cockroach neurons. NeuroToxicology 25, 967-980.

Zhao, X., Yeh, J.Z., Salgado, V.L., Narahashi, T., 2004b. Fipronil is a potent open channel blocker of glutamate-activated chloride channels in cockroach neurons. J. Pharmacol. Exp. Ther. 310, 192-201.

Zheng, Y., Hirschberg, B., Yuan, J., Wang, A.P., Hunt, D.C., Ludmerer, S.W., Schmatz, D.M., Cully, D.F., 2002. Identification of two novel *Drosophila melanogaster* histamine-gated chloride channel subunits expressed in the eye. J. Biol. Chem. 277, 2000-2005.

List of Publications

Chapter 2

Tomo Kita, Fumiyo Ozoe, Masaaki Azuma, Yoshihisa Ozoe, 2013. Differential distribution of glutamate- and GABA-gated chloride channels in the housefly *Musca domestica*. Journal of Insect Physiology **59**, 887-893.

Chapter 3

Tomo Kita, Fumiyo Ozoe, Yoshihisa Ozoe, 2014. Expression pattern and function of alternative splice variants of glutamate-gated chloride channel in the housefly *Musca domestica*. Insect Biochemistry and Molecular Biology **45**, 1-10.

List of related papers

Jia Huang, Hiroto Ohta, Noriko Inoue, Haruka Takao, Tomo Kita, Fumiyo Ozoe, Yoshihisa Ozoe, 2009. Molecular cloning and pharmacological characterization of a *Bombyx mori* tyramine receptor selectively coupled to intracellular calcium mobilization. Insect Biochemistry and Molecular Biology **39**, 842-849.

Yoshihisa Ozoe, Tomo Kita, Fumiyo Ozoe, Toshiyumi Nakao, Kazuyuki Sato, Kangetsu Hirase, 2013. Insecticidal 3-benzamido-*N*-phenylbenzamides specifically bind with high affinity to a novel allosteric site in housefly GABA receptors. Pesticide Biochemistry and Physiology **107**, 285-292.

Summary

L-Glutamic acid (hereafter glutamate) and γ-aminobutyric acid (hereafter GABA) are the major neurotransmitters. In invertebrates such as insects, these neurotransmitters mediate inhibitory neurotransmission by acting on specific ionotropic receptor (glutamate also mediates excitatory neurotransmission in invertebrates). Inhibitory glutamate receptor, glutamate-gated chloride channels (GluCls), are only present in invertebrates. Invertebrate GABA-gated chloride channels (GABACls) differ from mammalian ionotropic $GABA_A$ receptors in their subunit composition. Thus, these channels are the target of insecticides and anthelmintics; many studies about pharmacological properties of these channels using electrophysiological techniques have been performed. However, there are few reports about comparison between two similar ionotropic receptors in terms of physiological roles. Therefore in this study, I investigated channels gene expression levels and channel localization as a basis to understand differences in physiological roles using the housefly, *Musca domestica* L.

First, I investigated expression levels of genes encoding the housefly GluCl (MdGluCl) and Rdl (MdRdl) subunits by quantitative real-time PCR. Both channel subunit genes highly were expressed in the adult head. Interestingly, MdGluCl expression levels were higher than those of MdRdl in the adult legs. Next, I investigated the localization of both channels in the housefly using specific antibodies. Anti-MdGluCl staining was located in the optic lobe such as lamina, medulla, retina basement membrane and pigment cells in the adult head. Anti-MdRdl staining was located in medulla, lobula and lobula plate in the optic lobe, and antennal lobe and mushroom body where correlate with olfactory learning and memory. Differences in localization were observed in the adult thorax. MdGluCl was located in the cell surface of motor neuron cell bodies, whereas MdRdl was distributed in the neuropile of motor neurons in the thoracic ganglion. In addition, anti-MdGluCl immunoreactivity was distributed in the leg. These findings revealed that two similar inhibitory receptors function in different tissues.

MdGluCl gene has three splice variants termed *MdGluClA*, *B* and *C* generated by alternative splicing at exon 3. In addition, the MdGluCl gene has four RNA editing sites. I performed quantitative PCR and two-electrode voltage clamp (TEVC) experiments to investigate the gene expression and functional/pharmacological properties of variants. The MdGluClA and B transcripts highly were expressed in the adult head, while the MdGluClC transcript was expressed in the adult head and in the peripheral regions such

as legs and abdomen. These findings suggested that three splice variants differ in their expression levels and expression patterns; MdGluCls expressed in the leg may be MdGluClC channels. There was no significant difference in sensitivity to glutamate and the activator ivermectin B_{1a} when the variants were singly- or co-expressed in *Xenopus* oocytes. In contrast, MdGluClA and B channels were more sensitive to GABA receptor blockers fipronil and picrotoxinin (PTX), than MdGluClC channels. These results suggested that MdGluClA and B channels expressed in the central nervous system in the brain are sensitive to channel blockers than MdGluClC channels expressed in the peripheral tissues.

Antagonists that selectively act on GluCls are not known. Therefore, I tested some compounds known as GABACl noncompetitive antagonists against MdGluCl. Fipronil and PTX inhibited glutamate-induced currents, but sensitivities to GluCls were lower than to GABACls. Bicyclophosphorothionates, TBPS, PS-14, and 1HEPS, showed weak inhibition of three MdGluCl variants. Compounds that selectively act on GluCls were not identified in this study.

In conclusion, both GluCls and GABACls mediate inhibitory neurotransmission in invertebrates, but their localizations are different. Therefore, GluCls play different roles in the housefly body from GABACls. In addition, the *MdGluCl* gene has three splice variants, which differ in their expression levels and localization. These findings suggest that MdGluCl regulates inhibitory neurotransmission in different body part and tissues by splice variants.

要旨

グルタミン酸、γ-アミノ酪酸 (GABA) は代表的な神経伝達物質であり、昆虫などの無脊椎動物ではそれぞれが、特有のイオンチャネル型レセプターに結合することによりともに抑制性の神経伝達を行う (グルタミン酸は興奮性の神経伝達も行う)。抑制性グルタミン酸レセプターであるグルタミン酸作動性クロルイオンチャネル (GluCl) は無脊椎動物に特異的に存在している。また、無脊椎動物の GABA 作動性クロルイオンチャネル (GABACl) は哺乳類のものとは構造的に異なる部位がある。これらの点から両チャネルは殺虫剤や駆虫薬の作用点として知られている。そのため、電気生理学的手法を用いた薬理学的解析が数多く報告されている。しかし、類似した構造や機能を有する両チャネルの生理学的意義の違いについての報告は未だ少ない。そこで本研究では、両チャネルの生体内での役割の違いを解明するための基盤を得るために、衛生害虫であるイエバエ (*Musca domestica* L.) におけるチャネル遺伝子の発現量及びその局在を調べた。

まず､イエバエ GluCl サブユニットをコードする *MdGluCl* 遺伝子及び GABACl サブユニットである Rdl サブユニットをコードする *MdRdl* 遺伝子の発現量をリアルタイム PCR により調べた。その結果、両チャネル遺伝子は成虫イエバエ頭部において最も発現量が多いことがわかった。成虫脚における発現量は両チャネル遺伝子において違いが見られ、*MdGluCl* が *MdRdl* よりも多く存在した。次に両チャネルを特異的に認識する抗ペプチド抗体を作製し、生体内における両チャネルの局在を調べた。MdGluCl は成虫頭部ではラミナ、メダラ、網膜基底膜、色素細胞などの視覚葉に偏った分布を示した。一方 MdRdl は、成虫頭部ではメダラ、小葉、小葉板といった視覚葉全体に分布を示し、アンテナ葉、キノコ体などの嗅覚記憶に関与する領域も含め幅広い分布を示した。胸部においても両チャネルの分布には違いが見られた。MdGluCl は胸部融合神経節周辺に位置する運動ニューロンの細胞体膜に分布し、MdRdl は胸部融合神経節の運動神経網において分布していた。また脚では、MdGluCl の分布のみが確認された。これらのことから、両チャネルの生体内における役割は同じ抑制性の神経伝達であるが、働く部位が異なることが明らかになった。

MdGluCl 遺伝子にはエキソン 3 に 3 種類のスプライスバリアント (MdGluClA、B、C) が存在することが本研究で明らかになった。また、RNA 編集による影響を受ける部位が 4 箇所あることもわかった。これらの遺伝子多型がチャネル機能にどのような影響を及ぼすかを調べるため、スプライスバリアントに焦点を当て、イエバエにおけるそれぞれの遺伝子発現量及びチャネルの薬理学的解析

を二電極膜電位固定法 (TEVC) により調べた。その結果、*MdGluClA*、*B* は成虫頭部に偏った分布を示した。一方 *MdGluClC* は頭部においても発現が確認されたが、他の 2 種類とは異なり脚や腹部などの末梢神経系においても発現していることがわかった。これらのことから、3 種類のスプライスバリアントにはその発現量や発現部位に違いがあることが明らかになった。また、脚に分布していた MdGluCl は C タイプであることが示唆された。それぞれのチャネルの薬理学的性質を調べた結果、それらを単独発現及び共発現させた場合、グルタミン酸や作動薬であるイベルメクチン B_{1a} に対する感受性に差は見られなかった。しかし、GABA レセプターアンタゴニストであるフィプロニルとピクロトキシニン (PTX) に対する感受性は A、B の方が高く、C は低かった。これらのことから脳を含む中枢神経系に分布している A 及び B は薬剤に対する感受性が高く、一方末梢神経系においても分布している C は薬剤に対する感受性が低いことが示唆された。

GluCl は GABACl と比べて、特異的に作用する薬剤が少ない。そこで、既存の GABA レセプターアンタゴニストを用いて、GluCl においても作用を示すものがあるかを調べた。しかし、フィプロニルや PTX は作用を示したが GABACl よりも感受性が低く、他の薬剤はほとんど GluCl を阻害しなかった。これらのことから既存の薬剤では GluCl に選択的に作用するものは少ないと考えられる。

両チャネルは同じ抑制性神経伝達を行うが、発現部位に違いがあり、異なる抑制性神経伝達を行うことが示された。また、MdGluCl に存在する 3 種類のスプライスバリアントは発現量や発現部位が異なることから、部位による抑制性神経伝達をスプライスバリアントによって調節している